Effect of processing temperature profile during melt extrusion on thermoplastic starch production

Miguel Aldas[1], Cristina Pavon[2,*], Harrison De La Rosa-Ramírez[2], Juan López-Martínez[2] and Marina P. Arrieta[3,4]

[1] Departamento de Ciencia de Alimentos y Biotecnología, Facultad de Ingeniería Química y Agroindustria, Escuela Politécnica Nacional (EPN), 170517 Quito, Ecuador. (M.A. miguel.aldas@epn.edu.ec, ORCID: 0000-0003-3491-6618)

[2] Instituto de Tecnología de Materiales, Universitat Politècnica de València (UPV), 03801 Alcoy-Alicante, Spain. (C.P. cripava1@epsa.upv.es ORCID: 0000-0003-2902-0059, H.R.R. hardela@epsa.upv.es ORCID: 0000-0002-2913-7938, J.L-M. jlopezm@mcm.upv.es ORCID: 0000-0001-6904-2282)

[3] Departamento Ingeniería Química Industrial y del Medio Ambiente, Universidad Politécnica de Madrid, E.T.S.I. Industriales, 28006 Madrid, Spain. (M.P.A. m.arrieta@upm.es, ORCID: 0000-0003-1816-011X)

[4] Grupo de Investigación: Polímeros, Caracterización y Aplicaciones (POLCA), 28006 Madrid, Spain

***Correspondence:**

Cristina Pavon (cripava1@epsa.upv.es) (C.P.)

Laboratorio F3L5, Universitat Politècnica de València, Instituto Tecnológico de Materiales.

Campus Alcoy, Plaza Ferrándiz y Carbonell N°1, 03801 Alcoy (Alicante), Spain.

ABSTRACT

This work is aimed to evaluate the influence of the processing temperature on thermoplastic starch (TPS) for scalable production at the industrial level. Thus, it analyses the influence of six different extruding temperature profiles to plasticize native starch with water as well as with glycerol to obtain thermoplastic starch (TPS) produced by melt-extrusion. The temperature profiles ranged from 70 to 150 ºC. At temperature profiles below 100 ºC, the extrusion conditions were insufficient to disrupt the starch granules completely. Therefore, the material did not plasticize correctly, and the starchy matrix resulted in partially plasticized. by using a temperature profile of 100 ºC, the water evaporation process affects the final material's microstructure. At temperature profiles above 100 ºC (i.e.: 110 and 130ºC), the extrusion conditions allowed the disruption of the starch granule as well as a good material plasticization to obtain TPS. Although TPS obtained with a temperature profile of 150 ºC displayed the highest mechanical properties, the material shows signs of thermal degradation under these conditions. Therefore, TPS processed at profile with a maximum temperature of 130 ºC showed a higher plasticization effect, good thermal and mechanical properties, and good water uptake capability suggesting that TPS can be successfully obtained for their industrial production by processing native starch with water and glycerol at low share rates of 20 rpm and using 130ºC as a maximum processing temperature.

Keywords: thermoplastic starch, temperature profile, extrusion, plasticization, retrogradation

1. INTRODUCTION

Bio-based materials play an important role in helping conserve the environment, replacing non-degradable synthetic plastics with more friendly alternatives that could reduce the accumulation of plastic garbage due to lack of degradation or poor waste management (Ruhul Amin et al., 2020). Bio-based materials such as biofibers, bio-composites, and bioplastics are used as an alternative to synthetic plastics in different industrial products, mainly in short-term applications or disposable products such as the case of plastic bags, disposables (plates, cups, cutlery and straws), food packaging or agricultural mulch films (Vinod et al., 2020). In this regard, the European Commission specified that where sustainable alternatives are effortlessly accessible and affordable, single-use plastic products cannot be used (European Commission, 2023). Even though the European Commission encourages the use of recycled plastic in single-use products, the present legislation establishes stringent requests regarding food safety and for food contact materials does not permit the direct use of recycled plastics coming from recycled streams (European Commission, 2022). Therefore, fully biobased, and biodegradable plastics can be used in single-use products planned to be used in direct contact with food. Consequently, the production of food contact materials based on bioplastics is increasing. In this regard, bioplastics are materials produced from biomass, agro-resources, microorganisms, or synthesized from bioderived monomers (Vinod et al., 2020), for instance: cellulose (Gopi, Balakrishnan, et al., 2019; Gopi, Pius, et al., 2019; Rayón et al., 2013), alginates (Farokhi et al., 2019), proteins such as casein or caseinates (Arrieta et al., 2013), and starch (Aldas et al., 2021; Nevoralová et al., 2019; Pavon et al., 2021).

Currently, the biopolymer worldwide production is about 2.41 million tons and 18.7% of the total bioplastic production comes from starch (European Bioplastics, 2021) and it seems one of the furthermost promising bioplastics for outspreading bioplastics applications in food packaging and disposables. Starch is usually used as raw material for the development of biopolymers formulations as it is abundant in nature, inexpensive, comes from renewable sources, and due to its intrinsic biocompatible and biodegradable character (Ismail et al., 2017; Jiménez et al., 2012; X. Zhang et al., 2022). In general, bioplastics based on starch are used as blends with biodegradable polyesters (Ferri et al., 2018; Pattanayaiying et al., 2019), with synthetic polymers to add a grade of sustainability to

the final formulation as it is biobased and compostable (Sessini et al., 2019), as a matrix in biocomposites (Hassan et al., 2019; Jung et al., 2019; Rabe et al., 2019), and also in coatings and packaging developments (Arrieta et al., 2017; Gadhave et al., 2018). Additionally, there are commercial starch bioplastics such as Mater-Bi from Novamont, Bioplast from Biotec, Eslon Green and Greenpol from Yukong LTD (Bastioli, 1998; Mitrus & Wojtowicz, Agnieszka Moscicki, 2009), which have been blended with other natural additives to modify their properties (Aldas et al., 2019; Aldas, Rayón, et al., 2020; Scaffaro et al., 2018; X. Zhang et al., 2022).

Starch is a natural biopolymer synthesized by plants and some cyanobacteria whose main function is to store carbohydrates in spherical granules, whose size, quantity, and composition vary depending on the species that produce it (Apriyanto et al., 2022; Jiménez et al., 2012). The most common starch sources are cereal grains for instance barley, oat, wheat, and corn or potatoes and cassava tubers (Jumaidin et al., 2020). Structurally, starch is a semicrystalline polymer made up of two D-glucose homopolymers: amylose, usually a linear polymer with α (1 → 4) linkages, and amylopectin, with α (1 → 6) linkages which is highly branched (Apriyanto et al., 2022; Bertoft, 2017; Iaccheri et al., 2023). The content of amylose and amylopectin in the starch structure depends on various factors, for example the source of origin, age, or the extraction technique of the granules. It can be established that a common starch has amylose contents between 20 and 25 % and amylopectin contents between 75 and 80 % (Marichelvam et al., 2019). In its native state, starch is found as solid, insoluble granules, so for its processing, it is required to transform the granule to a fluid state (Xie et al., 2014). As reviewed by Jiménez *et al*. (2012), starch has been largely investigated for the development of edible and biodegradable films using the film formation method by solvent casting (Jiménez et al., 2012). Nevertheless, for its industrial uses, starch have to be transformed into thermoplastic starch (TPS), a polymeric material based on a starchy matrix with interest for the plastic processing industry. Since starch degradation temperature is inferior than starch melting temperature, to obtain a TPS, starch requires the action of heat and shear forces in addition to the incorporation of a plasticizer such as water, glycerol, or sorbitol (Xie et al., 2014; Y. Zhang, Rempel, & McLaren, 2014). As it was already commented, TPS can be obtained on a laboratory scale level through the solvent-casting method. However, for its industrial use, TPS has the advantage that it can be processed using the identical techniques employed for the processing of conventional polymeric systems, like extrusion or injection molding (Aldas, Pavon, et al., 2020b; Jumaidin et al., 2020; Mitrus, 2009; Oniszczuk & Janssen, 2009).

In the process of obtaining TPS, it should be considered that plasticizers are used to decrease the starch melting temperature and help destroy its crystalline structure (Montilla-Buitrago et al., 2021). It is worth mentioning that water helps to plasticize starch and prevents starch degradation during melt extrusion (Mitrus, 2009; Montilla-Buitrago et al., 2021). When the starch is heated together with a plasticizer, a phase transition in the starch structure is produced known as gelatinization, which involves a granule swelling, followed by a disruption of the crystal structure that will lead to the starch melting (H. Ma et al., 2022; Xie et al., 2014). On the other hand, shear forces, apart from producing a homogeneous blend, also cause the destructuration of the crystal structure. In addition, they can physically break the granules to allow plasticizers to enter the starch structure, affecting the final performance of the thermoplastic material (Xie et al., 2012). Thus, heating, shear forces, and plasticizers contribute to the starch melting process, successfully leading to TPS formation (Jumaidin et al., 2020).
Another factor to consider is that the temperature and the shear forces applied during melt extrusion can degrade the material (Wilpiszewska & Spychaj, 2006; Ye et al., 2018). The degradation degree will depend on a more significant measure of the processing parameters, for instance, the temperature profile used during the extrusion process and the rotation speed of the screws. Still, it also will depend on the composition and moisture content present in the material (Wilpiszewska & Spychaj, 2006; Xie et al., 2012). Although many authors stated that the processing conditions are of fundamental

importance in TPS production due to they can considerably affect the final performance of the starchy material, including the temperature profile and the moisture content (Toro-Márquez et al., 2018) there are no studies on the obtained properties of TPS-based materials as affected by different processing temperatures which are of a fundamental importance for the plastic processing industry.

In fact, the existing literature related to TPS extrusion processing focuses more on the study of the plasticizer's influence on the material properties (Montilla-Buitrago et al., 2021; Schmitt et al., 2015a; Yunos & Rahman, 2011; X. Zhang et al., 2022) and the impact of the extrusion variables (L/D ratio, shear force, rotational speed) (Artz et al., 1990; Souza & Andrade, 2002a; Thuwall et al., 2006; Ye et al., 2018), not so for the temperature influence. In these studies, glycerol is extensively used as a plasticizer, because of its availability, low cost, and high boiling point (290 ºC) (Kaseem et al., 2012). In this regard, it is well known that glycerol and water are good plasticizers because of their small molecular size, allowing them to easily enter the three-dimensional structure of starch (Montilla-Buitrago et al., 2021; Y. Zhang, Rempel, & Liu, 2014). Additionally, glycerol is a by-product of biodiesel manufacturing process and its use as plasticizer allows the revalorization of a low-grade by-product contributing to a circular economy (Arrieta et al., 2013). Corn starch is the type of starch most used for the TPS elaboration due to its high availability (Ciardelli et al., 2019), and since its high amylose content helps both in the starch gelatinization and the enhancement of the tensile properties of the biopolymers obtained, concerning TPS produced from low amylose starches (Marichelvam et al., 2019). However, it is worth to mentioning that Enrione et al. (2010) studied the glass transition temperature (T_g) of different sources of thermoplastic starches and no significant differences were observed in the glass transition temperature between extruded rice starches and waxy maize, nonetheless at high contents glycerol did form glycerol-rich zones in these polymeric systems which could affect the overall T_g of TPS (Enrione et al., 2010). Therefore, the glycerol plasticizer should be homogeneously distributed into the starchy matrix to achieve a good thermoplastic material.

As was previously commented, with the new legislation the production of TPS-based polymeric formulations is increasing in the industrial sector. Even more, the research regarding TPS production via thermoplastic extrusion is gaining great interest in the revalorization of wastes to obtain starch, as well as promoting new starch sources to fabricate thermoplastic starch. Costa et al. (2022) used modified loquat seed starch as a non-conventional source of starch to produce films for food contact applications, and the obtained films seemed to be interesting for low and medium water content foodstuff as kinds of pasta and baked food (Costa et al., 2022). Romeira et al. (2021) used potato starch acquired from potato washing slurries produced in a Food Company and revalorized it preparing thermoplastic starch films with an adequate cost and a potential application in film-forming solution for it use as papaya fruits coating (Romeira et al., 2021). Moro et al. (2017) mixed the residues of the passion fruit juice industry with starch in the film forming process by thermoplastic extrusion. It was determined that the residue added in 4 % enhanced the mechanical strength and Young's modulus and decreased the water vapor permeability (Moro et al., 2017). Therefore, to extend the applications of TPS-based products at the industrial level, it results of fundamental importance to understand the effect of processing temperature on the final overall performance of TPS-based materials.

Even though the processing temperature is known as a fundamental parameter to achieving gelatinization and granules melting, few studies have been published addressing the influence of different extrusion temperatures on TPS overall performance and as TPS production and use is rapidly increasing for single-use food contact materials applications it should be properly studied. Among them, there is a work done by Schmitt et al. in 2015, in which the effect of different plasticizers over the retrogradation of thermoplastic starch was analyzed. However, five different extrusion temperature profiles on TPS processing were used, 110–115–115 °C, 90–90–110 °C, 105–110–110

°C and 105–110–110 °C. Nonetheless, each temperature profile was used for processing material with different plasticizers: 110–115–115 °C for water and glycerol, 90–90–110 °C for sorbitol, and 105–110–110 °C for glycerol/sorbitol as well as urea/ethanolamine blend. As the primary objective of these studies was to analyze the effects of the used plasticizer, the temperature profile was not isolated, and there is no deeper analysis of the temperature profile used (Schmitt et al., 2015b). Pushpadass et al., in 2008, studied the effect of extrusion temperature on TPS processing. However, only two temperatures (110 °C and 120 °C) were investigated in this study. Furthermore, this parameter is not isolated since changes in TPS composition with different plasticizers were also analyzed (stearic acid, urea, and sucrose). Thus, it is concluded that TPS's physical and functional properties depend primarily on the type of plasticizer, without a clear conclusion on the processing temperature (Pushpadass et al., 2008).

Comentado [MA1]:

Comentado [MA2R1]: Ojo acá hay 4 perfiles de temperatura y 5 sistemas de plastificaión… he mirado el paper citado y está así!... he mirado otro paper de ellos: http://dx.doi.org/10.1016/j.carbpol.2012.04.03 y se procesa a 110-115-120 con glicerol y el blanco de agua…. ¿podemos asumir que el de sorbitol es el 90-90-110?

On the other hand, literature reports a wide range of TPS processing temperatures (from hopper to die) for TPS production used by different authors. For instance, Schmitt et al. (2015) work with wheat starch and blends of various plasticizers (i.e.: glycerol or sorbitol, as well as a blend of glycerol/sorbitol, or urea/ethanolamine blend), and in this work, different temperature profiles of 110, 115, 115 °C; 90, 90, 110 °C; 105, 110, 110 °C and 105, 110, 110 °C were used with an extrusion speed of 60 rpm (Schmitt et al., 2015a). Ghanbari et al. (2018) processed TPS from corn starch and glycerol with an extrusion speed of 80 rpm under the temperature profile of 80, 100, 110, 115, 120 °C, and 125 °C (Ghanbari et al., 2018). Mitrus (2005) studied TPS with potato starch and glycerol, and they used an extrusion temperature profile from 75 to 140 °C and a speed from 60 to 100 rpm (Mitrus, 2005). Wang and Huang (2007) processed TPS from corn starch using glycerol, and ethanolamine as plasticizers and they used a temperature profile of 110, 115, 120, and 125 °C and a speed of 20 rpm (Wang & Huang, 2007a). Souza and Andrade (2002) processed corn starch and glycerol with an extrusion speed from 20 to 40 rpm and a temperature profile of 70, 80, 95, and 115 °C (Souza & Andrade, 2002b). Liu et al. (2010) used a temperature profile of 50, 80, and 140 °C and a rotation speed of 180 rpm when working with corn starch, glycerol, and water (Liu et al., 2010). Van Soest et al. (1996) worked with a rising and falling temperature profile of 85, 140, 145, 120, 80, and 95 °C and an extrusion screw speed of 55 rpm. The final temperature was maintained below 95 °C to prevent water from boiling and obtain a non-porous material (Van Soest et al., 1996). In brief, most temperature profiles are established in rising order, with a gradual increase in temperature. In most cases, the intervals are between 5 and 10 °C, to avoid undesired effects such as changes in viscosity and degradation rate, which temperature variations could produce during extrusion (Liu et al., 2010). While the use of different temperature profiles is evident, no deep analyses of the effect of this processing parameter on the structure and overall performance of the obtained TPS have been reported. It can be concluded, that in most cases, the temperature processing conditions are determined from previously reported experiences as well as by trial-and-error practice during the processing of the materials until good quality TPS samples are obtained. Therefore, a deeper study on the effect of different processing temperatures is still a gap that needs to be filled for extending TPS production at the industrial level and its massive applications in single-use plastics. This study is intended to fill the gaps in deeper analyses of the influence of the processing temperature profile on the general performance of TPS obtained from corn starch and further plasticized with water and glycerol by the melt extrusion process. Glycerol was selected as it is food grade and the most used plasticizer for TPS production at the industrial level. A screw speed of 20 rpm was chosen to ensure that starch degradation due to high shear does take place, while the mixing time was 5 min. Then, six TPS-based formulations were prepared by melt extrusion using six different maximum processing temperatures of 70, 90, 100, 110, 130, and 150 ºC. The obtained formulations were characterized to get insights on the effect of processing temperature on the obtention as well as on the performance of TPS for their scalable production at the industrial sector. Thus, the paper analyzes obtained TPS's morphology, structure, mechanical and thermal, properties as affected by the processing temperature used. The optimal formulation was successfully obtained, and recommendations were made to

understand the processability of TPS made with starch, glycerol, and water in which the hydroxyl groups of glycerol destroy the original hydrogen bonds previously established in starch molecules between them and allow to obtain starchy matrix in its thermoplastic form showing it potential industrial scalability.

2. MATERIALS AND METHODS

2.1. Materials

Food-grade corn starch composed of 27% amylose, provided by Cargill (Barcelona, Spain), was used to elaborate TPS. Glycerol with a purity of 99% provided by Panreac (Barcelona, Spain) and distilled water were used as plasticizers. Glycerol was added at 25 wt.% and water at 10 wt.% of the total blend. Then, the materials were manually premixed in an airtight polyethylene bag. They were stored for 24 hours to ensure the plasticizers, water, and glycerol entrance into the starch granules (Oniszczuk & Janssen, 2009).

2.2. Thermoplastic starch processing

Before extrusion, the blend was stirred to guarantee material homogeneity and regular feeding (Oniszczuk & Janssen, 2009). The blend was processed at 20 rpm by means of a co-rotating twin-screw extruder with an L/D ratio of 25 from Dupra S.L (Castalla, Spain). For the study, five different temperature profiles were used, which were varied in steps of 20 °C between each profile. In addition, a profile was used to verify the behavior of TPS at the water boiling temperature (100 °C). The samples were labeled according to the maximum temperature used in the profile, and the corresponding extrusion profiles used are listed in Table 1~~Table 1~~.

Con formato: Fuente: Sin Negrita

Table 1. Label of the TPS studied materials according to the extrusion temperature profile

Sample label	Extrusion temperature profile (ºC)			
	Zone 1 (Die)	Zone 2	Zone 3	Zone 4 (Feeding hopper)
T70	70	60	50	40
T90	90	80	70	60
T100	100	90	80	70
T110	110	100	90	80
T130	130	120	110	100
T150	150	140	130	120

The die of the extruder was a round sheet with holes of a diameter of 3.5 mm. After extrusion, filaments with diameters between 3 and 4.5 mm were obtained. The filaments were used for the respective characterizations. Since the environmental conditions influence TPS-based materials' properties, the obtained starchy samples were kept at 25 °C and 50 ± 5% HR immediately after extrusion and before being characterized (Aldas et al., 2019).

2.3. Thermoplastic starch characterization

2.3.1. Visual and optical characterization

The color, surface appearance, and diameter of the obtained filaments were evaluated for visual and optical characterization. Additionally, the materials were observed in an Olympus optical microscope,

model SZX7 from Olympus Iberia (Barcelona, Spain), and photographed with the help of a digital microscopic camera. The surface appearance of the filaments was visually examinated. Diameters were measured with an electronic digital caliper, model Pro-Max, from Fowler High Precision (Newton, Massachusetts, USA). The color was measured on a Colorflex-Diff2 458/08 colorimeter from HunterLab (Reston, VA, USA) using the CIEL*a*b* space by determining L *, a *, and b * coefficients. For diameter and color evaluation, for each sample ten different measurements were performed, and the mean a values were reported with the corresponding standard deviation. The significant differences were statistically analyzed with the one-way analysis of variance (ANOVA), using OriginPro 8 software, at a 95% confidence level according to Tukey's test for the significant differences among starchy samples.

2.3.2. Microstructural characterization

Field Emission Scanning Microscopy (FESEM) was carried out on a Zeiss Ultra 55 microscope at 1 kV over the surface of the filaments. Before the analysis, the obtained filaments were cryo-fractured and covered with a layer of gold-palladium alloy by means of a Sputter Mod Coater Emitech SC7620, Quorum Technologies (East Sussex, UK) to allow electrical conduction.

X-ray Diffraction (XRD) was used to study the crystallinity variations in the thermoplastic starch structure due to the changes in the processing temperature profile. X-ray Diffraction patterns were obtained using a Bruker D8 Advance X-Ray Diffractometer with a linear detector Lynxeye XE. The scattering angles (2θ) used was from 4° to 50° at a rate of 1°/min. The measurements were performed using a 1 mm thick sample with a smooth surface.

Attenuated total reflectance–Fourier transform infrared spectroscopy (FTIR-ATR) was employed to analyze the molecular interactions of TPS components and their changes due to the processing temperature profile. The analysis was done at ambient temperature in transmission mode in a Nicolet iS10 FTIR spectrometer (Thermo Scientific, Waltham, MA, USA) coupled with a Smart iTX ATR accessory. The measurements were performed within 4000–600 cm^{-1} at a resolution of 16 cm^{-1} and 16 scans.

2.3.3. Mechanical characterization

Tensile test measurements were carried out on an Ibertest Elib 30 SAE Ibertest (Madrid, Spain) universal testing machine following ISO 527 standard [42], with a 5 kN load cell and a speed of 10 mm/min. Extruded filament samples of 80 ± 1 mm in length and constant diameter were used as test specimens with a grips distance of 50 mm. Young's modulus, tensile strength, and elongation at break were determined by the average of five measurements. The significant differences were statistically calculated with the same parameters previously described. Additionally, the toughness of each TPS was obtained from the area under the typical stress–strain curve. The area was calculated using the OriginPro2015 program. The mean value and the standard deviation for each sample are reported.

2.3.4. Thermal characterization

Thermogravimetric analysis (TGA) was conducted on a TGA Q500 TA Instruments thermal analyzer (Selb, Germany). A dynamical analysis was carried out from 35 °C to 700 °C with a heating rate of 10 °C/min using nitrogen with a 30 mL/min flow rate as circulating gas. The onset decomposition temperature was determined when the materials lost 5% of their weight ($T_{5\%}$). The end decomposition

temperature is when the materials lose 90% of their initial weight ($T_{90\%}$). The maximum decomposition rate temperature (T_{max}) was defined at the minimum of the first derivative of the TGA curve (DTG).

Differential scanning calorimetry (DSC) was conducted on Mettler DSC821e equipment (Toledo, Spain). The samples were analyzed using a dynamic thermal cycle consisting of a heating step from -50 °C to 170 °C, followed by a cooling step to -50 °C, and second heating from - 50 °C to 170 °C. In all the steps the speed was 10 °C/min and a nitrogen atmosphere (flow of 30 mL/min) was used. Glass transition temperatures (T_g) were evaluated on the second heating curves.

Dynamic Mechanical thermal analysis (DMTA) was conducted in DMA1 Mettler-Toledo (Schwerzenbach, Switzerland) using filaments of constant diameter as samples. The analysis was carried out using a single cantilever mode and a maximum deformation of 10 µm. The samples were analyzed within −100 up to 100 °C with a heating rate of 2 °C/min and a frequency of 1 Hz.

2.3.5. Water uptake

The water uptake test was performed following ISO 62 standards (International Standards Organization, 2008). The test was carried out on extruded filament specimens of 25 ± 1 mm in length and constant diameter. The initial weight (W_1) was determined by drying the samples at 50 °C for 48 h. Then, each sample was placed in a container with 300 mL of distilled water at room temperature. To plot the change in sample weight over time due to water absorption, the samples were weighed every 15 min during the first hour, then every 30 min until 3 hours of testing, and every hour until 8 hours of testing. For each measurement, the specimens were taken out from the water; the surface water was withdrawn with filter paper and weighed again (W_2). The water absorption (c) at each point was determined with equation 1. Three specimens of each material were tested. The mean values were reported with their corresponding standard deviation of the, and the significant differences were statistically calculated with the same parameters previously mentioned.

$$c = \frac{W_2 - W_1}{W_1} \times 100 \quad (1)$$

3. RESULTS

3.1. Thermoplastic starch formulations, processing, and visual characterization

It is known that starch can exhibit thermoplastic properties when it is processed with plasticizers, applied shear, and at elevated temperatures. In the present work, glycerol was selected as plasticizer as it is the most widely used plasticizer for TPS production at the industrial level, it is food-grade, and it is currently obtained as a by-product during biodiesel manufacturing. Therefore, from a circular economy point of view, the use of glycerol as a plasticizer allows for increasing its added value from a low-grade by-product to a plasticizer for sustainable biopolymeric formulation production (Arrieta et al., 2013). Glycerol and water are considered the most effective plasticizers for TPS production mainly because of their small size as well as their hydrophilic nature which make them compatible with the starch matrix allowing ease of penetration within the three-dimensional starch networks (Pushpadass et al., 2008). As glycerol is widely used in TPS production, the percentages of glycerol and water were established in this work according to the literature. In this sense, Wojtowicz et al. (2009) have proven that 25 wt% of glycerol is enough to achieve complete gelatinization of the starch. While minor contents than 25 wt% do not produce a complete plasticization, with higher contents, a

migration of glycerol occurs (Oniszczuk & Janssen, 2009). Furthermore, water was added at 10 wt% since Liu et al. (2010) showed that adding water to the blend aided the gelatinization and prevents the degradation of the starch granules (Liu et al., 2010; Y. Zhang, Rempel, & Liu, 2014). To avoid thermomechanical degradation of TPS polymer in the melt extrusion, since starch degradation temperature is lower than its melting temperature, not only the temperature profile should be carefully selected, but also screw speed as well as mixing time.

In this work, before processing, the materials were manually premixed in sealed plastic bags and then allowed to rest for 24 hours to promote the entrance of both plasticizers, water, and glycerol. The obtained swelled mixtures of starch, glyecerol and water were then fed into the extruder and processed at a screw speed of 20 rpm to avoid starch degradation due to high shears, while the mixing time was 5 min. The appearance of the different filaments obtained as well as the optical micrographs are presented in Fig 1~~Fig 1~~ and, Table 2~~Table 2~~.

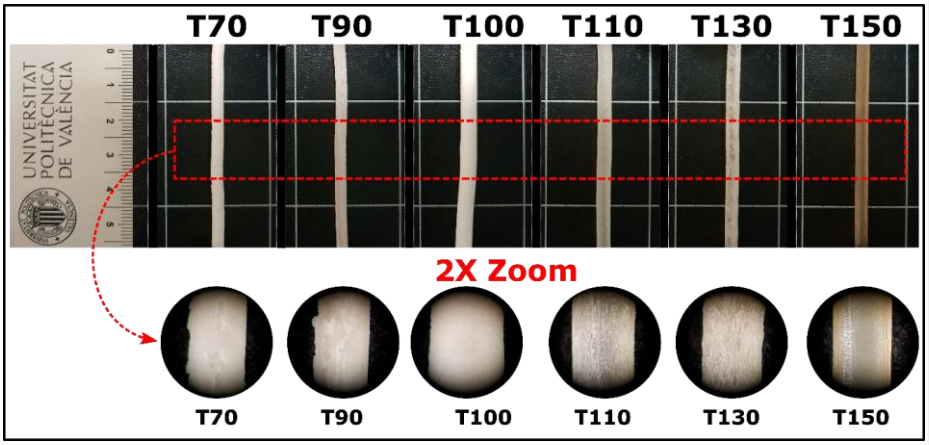

Fig 1 Visual appearance and microscopic view (1.6X) of TPS filaments obtained at different temperatures at a screw speed of 20 rpm

Table 2. Visual characterization results of the obtained filaments

Sample label	Filament diameter (mm)	Superficial appearance	Color			
			L*	a*	b*	YI
T70	3.2±0.1[a]	Matte, rough, heterogeneous surface with scales and opaque	73.0±1.1[a]	0.4±0.1[a]	9.4±0.5[a]	22.7±1.1[a]
T90	3.1±0.1[a]	Matte, rough, heterogeneous, and opaque surface with scales	63.6±0.6[b]	0.8±0.1[a]	9.5±0.2[a]	26.0±0.7[b]
T100	4.4±0.1[b]	Matte, smooth, homogeneous, and opaque surface	81.3±1.8[c]	-0.7±0.1[b]	9.6±0.4[a]	18.6±0.4[c]
T110	3.7±0.1[c]	Matte, rough, homogeneous, and translucent surface	46.4±0.6[d]	-1.7±0.2[c]	7.9±0.6[b]	24.8±1.3[a,b]

T130	3.5±0.1[d]	Matte, rough, homogeneous, and translucent surface with scales	51.1±1.1[e]	-0.5±0.8[b]	8.7±0.4[a,b]	25.3±2.0[b]
T150	3.6±0.1[d]	Shiny, smooth, homogeneous, and translucent surface	32.9±0.6[f]	2.5±0.2[d]	12.2±0.7[c]	55.4±1.3[d]

a–f Different letters within the same property indicate statistically significant differences between materials ($p < 0.05$).

The diameters of the filaments processed at low (T70, T90) and high temperatures (T130 and T150, respectively) do not show significant differences among them ($p > 0.05$). The filaments processed at temperatures below 100 °C have a smaller diameter than those processed at 100 ºC or high temperatures. It is also observed that the filament processed at 100 °C presents the largest diameter of all the studied materials (4.4 ± 0.1 mm). This behavior is because, at this temperature, the water present in the blend evaporates just as the filament leaves the extruder, which causes the swelling of the material, and therefore the diameter increases, as was observed by Mitrus (Mitrus, 2009). Regarding the surface appearance of the filament and the color, it is observed that the processed materials at temperatures below 100 °C (T70 and T90) present a heterogeneous surface, which suggests a poor and/or heterogeneous plasticization of the starch matrix (Fig 1~~Fig 1~~ and Table 2~~Table 2~~), and there is also a color change in these filaments. For the T100 material, the L* coordinate, which indicates the material luminosity, has a value of 81.3 ±1.8, so the filament is seen in white tones. This change in color and the smooth appearance of the filament are due to water evaporation. For T130 the luminosity shows a reduction on the L* coordinate concerning T100, but significantly higher than T100, suggesting intermediate lightness between these two samples. Meanwhile, the color is mainly similar to that of T110 since they showed similar values of b* coordinate and YI ($p > 0.05$), indicating to a certain degree a trend to yellow. However, in the case of T150 materials, which represents the highest temperature used here, the smooth appearance of the surface may suggest the beginning of a degradation process due to the high processing temperature used, which is corroborated by the color change. For this sample, the coordinates a* and b* tend to have higher positive values, so the material is appreciated with a brown hue. In addition, the yellowing index increases significantly ($p < 0.05$) from YI = 25 (in the previous processing temperature of 130) to YI = 55 (in T150), suggesting that the material suffered thermal degradation during processing. Finally, a reduction in the L* value shows a loss of clarity (luminescence) which suggest a recrystallization of the starch.

Con formato: Revisar la ortografía y la gramática

3.2. Microstructural characterization

The morphological changes on the TPS matrix as a consequence of the different processing temperatures were investigated by FESEM and Fig 2~~Fig 2~~ displays the FESEM micrographs of the cry-fractured cross-section of all samples in which it is possible to analyze the morphology of native corn starch granules of the different processed starchy materials. Fig 2~~Fig 2~~-a shows the corn starch granules, whose morphology and size (between 5 and 12 µm) agree with that reported in the literature (Wilpiszewska & Spychaj, 2006; Xie et al., 2014; Y. Zhang, Rempel, & Liu, 2014). T70 and T90 (Fig 2~~Fig 2~~-b and Fig 2~~Fig 2~~-c) presented two phases within the same material, a continuous phase formed by the plasticized starch granules and a dispersed phase consisting of whole or partially broken starch granules (X. Ma & Yu, 2004; Yang et al., 2006; Zullo & Iannace, 2009). The presence of the unbroken granules shows that the maximum temperatures of 70 ºC and 90 ºC, used in the temperature profiles for processing T70 and T90, respectively, are not enough to lead to a complete disruption of the starchy granule. Therefore, the plasticizer cannot fully enter the starch granular structure, and the transformation process from starch to TPS is not successfully completed (Xie et al., 2012).

On the other hand, T100 (Fig 2~~Fig 2~~-d) displays a porous structure produced by the boiling and evaporation of water contained in the initial TPS formulation (Mitrus, 2009). Meanwhile, T110 (Fig

2Fig 2-e) presents a ductile fracture surface with a few holes suggesting the presence of starch granule residues. Thus, the images suggest that T100 and T110 structures are partially plasticized. Quite the opposite, T130 (Fig 2Fig 2-f) presents a smooth and soft surface where starch granules cannot be distinguished, showing a material free of defects. Arredondo-Ochoa et al. (2017), studied edible films of oxidized corn-starch plasticized with sorbitol prepared by solvent casting method and observed similar compact structure (Arredondo Ochoa et al., 2017). In the current work, the homogeneous material obtained at this temperature (T130 ºC) indicates that a good combination of temperature and shear force in the extrusion process was achieved, allowing a better granule disruption (Zullo & Iannace, 2009). In this way, a strong interaction between starch, glycerol, and water occurs, producing adequate material plasticization at a maximum temperature of 130ºC Similar findings were observed by Ma and Yu who prepared formamide/glycerol plasticized TPS (X. Ma & Yu, 2004). However, it should be mentioned that although amide groups have shown their effectiveness for plasticizing starchy matrix as a consequence of the electronegativity of their functional groups, they are not useful for food contact materials due to their toxicity (Montilla-Buitrago et al., 2021).

When T150 was used, the material (Fig 2Fig 2-g) exhibits cracks and new structures on the material surface (expanded area Fig 2Fig 2-g), which indicates a stiffening of the material microstructure. This behavior is ascribed to thermal degradation during extrusion due to the high temperature of the process, which affects amylopectin molecules to the greatest extent (Stepto, 2006a; Xie et al., 2014). In this condition, the amylopectin chains interact among them, which causes recrystallization on cooling, resulting in a more rigid and crystalline structure (Hoover, 2001; Paridah et al., 2016). Furthermore, the high temperatures to which the starchy material is subjected may be breaking the amylose chains, which would facilitate a rearrangement of the chains upon cooling (Y. Zhang, Rempel, & Liu, 2014). Additionally, the material color change previously commented (see T150 in Fig 1Fig 1) suggests that thermal degradation had taken place in T150 which confirms the retrogradation (recrystallization) phenomenon (Paridah et al., 2016; Stepto, 2006b). Other works also observed these crystalline structures when studying a Mater-Bi type bioplastic that it is a commercial thermoplastic based on a thermoplastic starch matrix widely used in the bioplastic processing industry (Aldas, Rayón, et al., 2020).

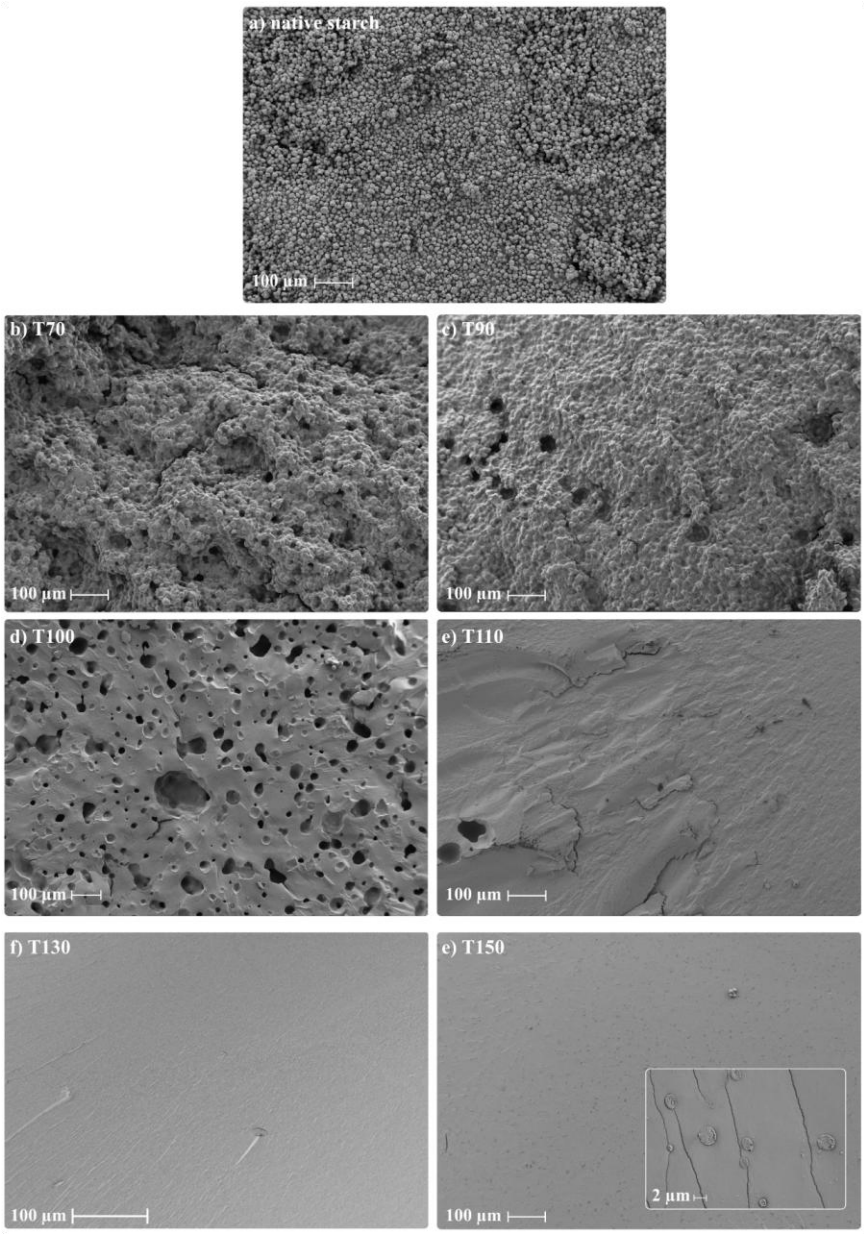

Fig 2 a) Corn starch granules and TPS obtained at different processing temperature profiles: b) T70 °C, b) T90 °C, d) T100 °C, e) T110 °C, f) T130 °C and g) T150 °C

The X-ray diffraction (XRD) patterns obtained for all thermoplastic starch materials prepared at different temperature profiles are presented in Fig 3~~Fig 3~~ with native corn starch XRD pattern for comparison. Native corn starch XRD pattern shows a type A crystallinity typical of cereals, characterized by a strong intensity peak at 2θ = 15.2°, a double peak at 2θ =17.2° and 18.1°, and another strong intensity peak at 2θ = 23° (Angellier et al., 2006). After the extrusion process, the crystalline structures of native starch change with all the temperature profiles since the shape of all peaks change from an A-type crystallinity to a V-type crystallinity, and the halo of the curve is modified. It is seen that the crystallinity of the samples significantly decreases concerning native corn starch due to the granular disruption of starch as a consequence of the extrusion process (Angellier et al., 2006; Castillo et al., 2019). The V-type crystallinity in TPS, in which natural crystals have been mainly destroyed by the combination of temperature and shear forces is produced because starch chains compounded with glycerol and water can crystallize during hot-melt extrusion (Chen et al., 2020). Moreover, it is seen that the crystalline peaks and the amorphous halo of thermoplastic starch are dependent on the processing temperature. T70 presents similar peaks to those of native starch, at 2θ =15°, a double peak at 2θ = 17° and 18°, a peak at 2θ = 23°, as well as a new low-intensity peak centered at 2θ = 19.7° associated to crystallinity induced during processing (V_H-subtype) (Chen et al., 2020). In the XRD of T90, low-intensity peaks of V_H- subtype crystal structure (12.6°, 19.6°, and 22.4°) formed by the crystallization of amylose during hot-melt extrusion or during cooling are observed. However, residual A-type crystallinity peaks are still seen at 15° and 17.2° due to non-plasticized starch. Therefore, temperature profiles of 70 °C and 90 °C are not enough to completely disrupt native corn starch granules, which confirms the results obtained by the SEM characterization. T100, T110, and T130 display V_H-type peaks at 2θ = 12.6°, 19°, and 22° and present the typical amorphous halo of semicrystalline thermoplastic starches, centered on 19° (Campos et al., 2013a; Ostafińska et al., 2017). Besides, the absence of A-type crystal peaks confirms that the starch structure was completely destructured in these TPSs (Mendes et al., 2016). The intensity in the V_H-type peak centered at 19.7º could be related to the progress in the formation of thermoplastic starch. T70 and T90 present a low-intensity peak which indicates incomplete plasticization, T100, and T110 present a medium-intensity peak indicating that the material is plasticizing to form TPS, T130 displays a high-intensity peak showing further plasticization and formation of the TPS structure. Finally, T150 presents a shift of the peaks to 18º and 21º which may be pointing to a transition to an A-type structure due to retrogradation (Lendvai et al., 2019). Besides, the XRD pattern of T150 has a significant reduction of the amorphous fraction of TPS since the amorphous halo is almost flat, which shows that this material is more crystalline than those obtained at lower temperatures. This behavior agrees with the SEM observations, where the material's recrystallization was inferred due to the thermomechanical degradation in the extrusion process. Moreover, T100, T110, and T130 XRD patterns have a peak at 16.8°, which is associated to the recrystallization of short chains of amylopectin produced by short-term aging (B-type crystallinity) (Campos et al., 2013b).

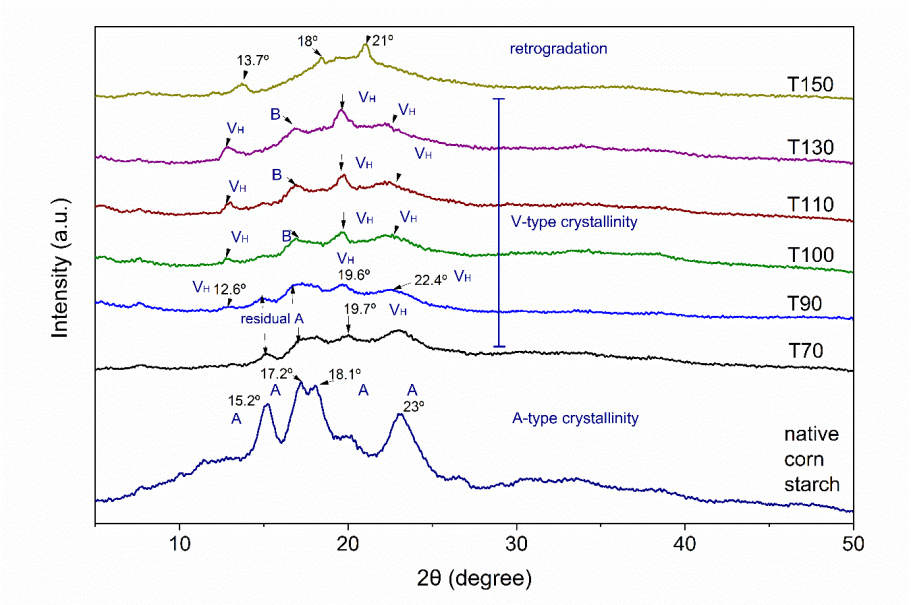

Fig 3 X-ray diffraction patterns of native corn starch and thermoplastic starch (TPS) processed at different temperature profiles T70, T90, T100, T110, T130, and T150

The FTIR spectra of thermoplastic starches processed at different temperatures are plotted in Fig 4~~Fig 4~~. Changes in the spectra are found in the O-H stretching and -C-H stretching groups Fig 4~~Fig 4~~-b. The O-H stretching, typically located at around 3300 cm^{-1} in TPS-based materials (Romeira et al., 2021)is located at 3283 cm^{-1} in T70, at 3325 cm^{-1} in T 90 and T100, at 3338 cm^{-1} in T110 and T130, and 3340 cm^{-1} in T150. It seems that the wavenumber of O-H stretching increases from T70 to T150. Moreover, the intensity of the -C-H stretching band located at 2928 cm^{-1} increases with temperature. The growth in the intensity -C-H band accompanied by the shift of -O-H wavenumber with increasing temperature can suggest that the hydrogen bond between starch becomes weaker as new bonds are formed due to the plasticization. The intensity of the -O-H peak increases when increasing temperature from 100ºC to 130 ºC. This behavior shows that the rise in temperature to higher values than 100ºC (i.e., T110 and T130) enhances the interaction between the plasticizer and the hydroxyl groups, allowing –OH groups from glycerol to destroy the original hydrogen bonding interactions between starch molecules, which in turn make it thermoplastic (Shi et al., 2007). In T150, the intensity of the peak decreases which is accompanied by the shift of the peak to a higher frequency suggesting a decrease of the average strength of the hydrogen bonds as well as a broadening of the distribution (Dang & Yoksan, 2015). Regarding the fingerprint region of the spectrum three characteristic peaks appeared between 1200 and 900 cm^{-1}, ascribed to the C-O bond stretching of starch: at 1150 cm^{-1} there is a peak attributed to the C-O bond stretching of the C-O-H group in starch. There are two additional peaks at 1080 and 1020 cm^{-1} which are ascribed to C-O bond stretching of C-O-C group in the anhydroglucose ring (X. Ma et al., 2007). Ma et al (2007) studied starch plasticized with different plasticizers and attributed the shifts of the C-O bond stretching peaks to the interaction

between starch and plasticizers (X. Ma et al., 2007). According to Pawlak and Mucha (2003), the lower the peak frequency the stronger the interaction (Pawlak & Mucha, 2003). In Fig 4~~Fig 4~~-c it is shown that T110, T130, and T150 have a stronger interaction with the plasticizer with respect T70, T90, and T100. The three TPS samples have a higher wavenumber (lower frequency) than 1120 cm^{-1}. Nevertheless, T130 presents the highest wavenumber (1125 cm^{-1}) which indicates the best interaction between starchy polymeric matrix and glycerol.

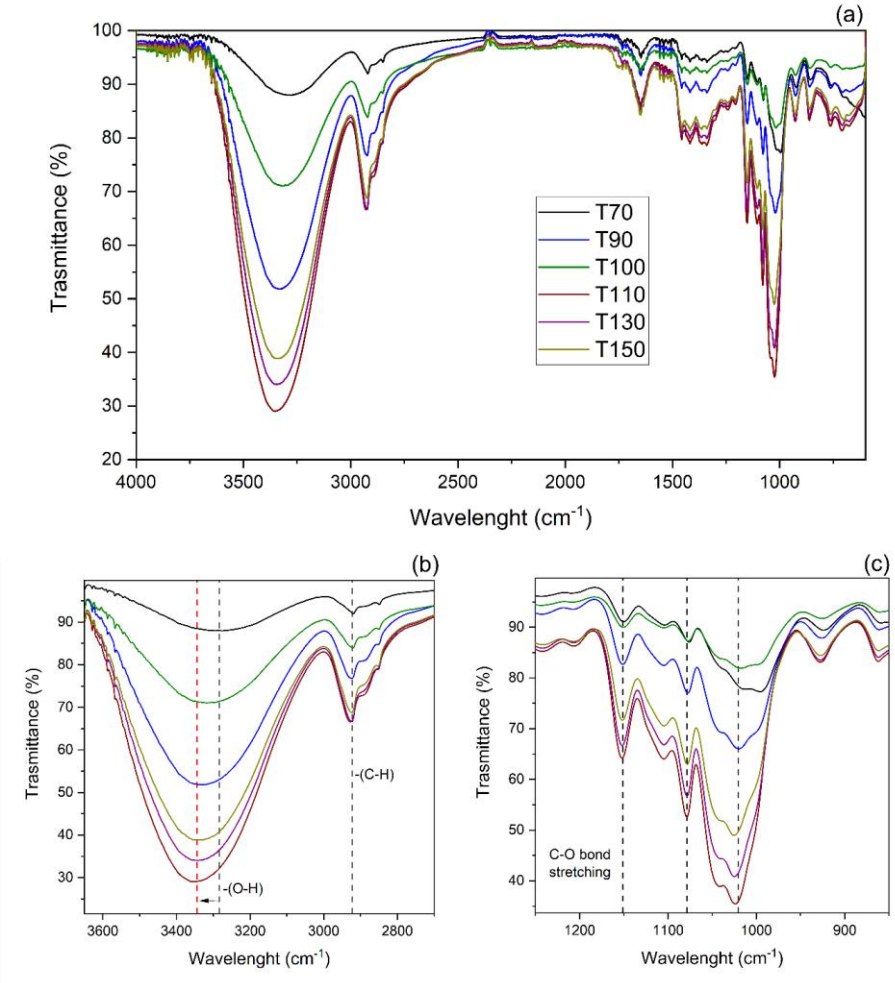

Fig 4 (a) FTIR spectra of thermoplastic starch (TPS) processed at different temperature profiles T70, T90, T100, T110, T130, and T150 (b) expanded area of -O-H stretching and -C-H stretching groups and (c) expanded area of C-O bond stretching

3.3. Mechanical characterization

The materials mechanical resistance is of a fundamental importance in materials to be used infood packaging due to they are required to protect the foodstuff from the surrounding during transport and storage. Table 3~~Table 3~~ shows the mechanical properties obtained from the tensile strength test. In Fig 5~~Fig 5~~ it can be seen the typical stress-strain curve for the different studied starchy materials. Regarding Young's modulus, materials T70, T90, and T150 present a modulus of up to six times greater than T100, T110, and T130. In T70 and T90, this stiffening effect is produced by the presence of the unplasticized starch granules in the TPS polymeric matrix, as verified through SEM micrographs (Fig 2~~Fig 2~~-a and Fig 2~~Fig 2~~-b). These starch granules could act as fillers, thus reinforcing the polymeric matrix. Sessini et al. (2016) studied TPS reinforced with starch nanoparticles in this sense the starch-based nanofillers reinforce the TPS matrix due to nanoparticles and matrix good interaction (Sessini et al., 2016). In the present work, the good interaction between unplasticized starch granules and the TPS polymeric matrix increases the elastic modulus value. However, the granules also constitute stress concentration points (physical joints) in T70 and T90 materials which also produce a decrease in the flexibility and the resistance of thermoplastic starch, as can be seen in the tensile strength and elongation at break values (Table 2) which resulted in the lowest when are compared to the materials processed at higher temperatures.

Table 3. Tensile properties of the TPS obtained at different temperatures.

Sample label	Young's modulus (MPa)	Tensile strength (MPa)	Elongation at break (%)	Toughness (kJ/m^3)
T70	12.6 ± 1.5^{a}	0.17 ± 0.11^{a}	4.5 ± 1.8^{a}	7 ± 3^{a}
T90	20.4 ± 1.9^{b}	0.42 ± 0.03^{b}	5.5 ± 0.4^{a}	12 ± 1^{a}
T100	5.1 ± 0.3^{c}	0.45 ± 0.03^{b}	22.2 ± 2.1^{b}	60 ± 2^{b}
T110	4.4 ± 0.3^{c}	0.95 ± 0.11^{c}	34.4 ± 6.3^{c}	304 ± 14^{c}
T130	5.2 ± 0.7^{c}	0.82 ± 0.06^{c}	70.1 ± 4.3^{d}	380 ± 53^{d}
T150	32.2 ± 2.7^{d}	3.28 ± 0.20^{d}	169.5 ± 30.1^{e}	4832 ± 535^{e}

[a-d] Different letters within the same property show statistically significant differences between formulations ($p < 0.05$)

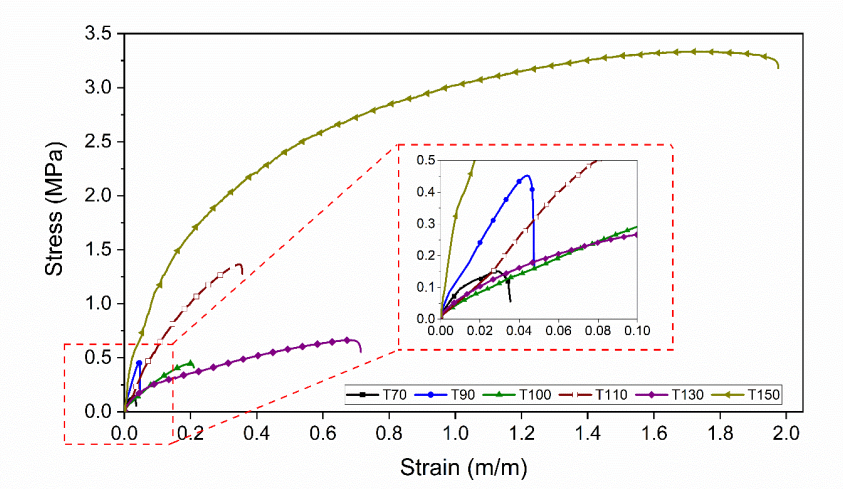

Fig 5 Typical stress-strain curve of filaments of TPS obtained at different processing temperatures profiles

T100 displayed a low Young's modulus and tensile strength, which are attributed to the porosities observed in the microstructural characterization of this material, caused by the water evaporation from the blend when the material was extruded, as was verified in the SEM analysis (Fig 2~~Fig 2~~-d). These pores act as stress concentrators, which lead to a material with low tensile strength and, in general, poor overall mechanical performance (Mitrus, 2009). However, the significant increase in the elongation at break in T100 with respect to T70 and T90, indicates that the material has begun to plasticize. T110 and T130, also present a progressive intensification in the elongation at break values pointing to a greater plasticization. The elongation at break of T130 is statistically greater ($p < 0.05$) than the elongation at break of T100 and T110, indicating greater cohesion of the structure and therefore higher plasticization. Moreover, no significant differences ($p > 0.05$) were found for Young's modulus of T100, T110, and T130. Tensile strength significantly increases in T110 and T130 with respect T100, indicating better cohesion due to the absence of holes and higher cohesion.

It is known that the mechanical properties of starchy materials are dependent on the interaction between the polymeric matrix and the additives used, achieving a good plasticization effect when good flexibility, low brittleness, as well as improved stretching ability are obtained (Arredondo Ochoa et al., 2017). The similarity in the mechanical properties' values (Table 2~~Table 2~~) and the changes in the microstructure seen in the SEM micrographs (Fig 2~~Fig 2~~) indicate that the materials begin to plasticize at temperatures of 100 °C. These processing conditions allow the starch granules to be broken by the shear action due to the extrusion process and the temperature, which causes the disruption of the starch granules producing a greater interaction with the plasticizer and allowing a better plasticization (Paridah et al., 2016; Van Soest et al., 1996).

Con formato: Revisar la ortografía y la gramática

T150 seems to have the best mechanical properties among all the studied samples, showing much higher modulus values, tensile strength, and elongation at break. SEM micrographs (Fig 2~~Fig 2~~) of T150 exhibit crystalline domains, which increase the mechanical properties of the starchy material. Conversely, as the material suffers thermal degradation during the extrusion process at so high-temperature conditions, the resultant material is a highly plasticized starch with crystalline structures

inside. Moreover, within T150, shorter starchy polymeric chains are generated because of the polymer thermal degradation, these chains contribute to the maximum elongation at break of these materials. On the other hand, crystalline structures act as reinforcing elements. According to Aji P. et al. (2002), there is also a crosslinking effect (between the amorphous and crystalline parts) that improves the material mechanical properties (Mathew & Dufresne, 2002). Consequently, when T150 is exposed to tensile deformation, the crystalline domains, and polymer chains are reoriented in the direction of the applied stress, and strain hardening occurs. As a result, the material toughness increases (Paiva et al., 2018). Table 3~~Table 3~~ displays the toughness values of the materials T150 has the highest toughness due to the strain hardening. Moreover, T130 has a higher toughness than T110, indicating a higher plasticization for T130. Meanwhile, the lowest toughness value is reported for T70 and T90, due to the plasticization failures.

Fig 5~~Fig 5~~ shows an average stress-strain curve of the studied blends. In the graphic it is observed that T110 and T130 present close toughness values, it can be verified that the plasticizing effect can be seen in the shape of those curves. However, T130 has higher elongation, which is typical of a plasticized material. T100 also has a characteristic stress-strain curve of a plasticized material. However, the presence of porosities in the material detracts from the properties of the TPS. Finally, T150 also showed the typical stress-strain curve of plasticized starch. In this way, it can be said that at temperatures greater than 100 °C, under the processing conditions described in this study, starch can be plasticized, presenting partial plasticization at T100 and T110, and high plasticization at T130 and T150. Nonetheless, even when T150 presents good overall tensile properties it shows signs of thermal degradation.

3.4. Thermal characterization

Fig 6~~Fig 6~~ compares the thermal decomposition curves of TPS processed at different temperatures and pure starch. For all the analyzed materials, the thermal degradation curve (TGA) presents three decomposition stages (Fig 6~~Fig 6~~-a). In the case of pure starch, according to Paridah et al. (2016), the first stage occurs up to 120 °C and matches to the loss of free water in the starch (Paridah et al., 2016). In the starch curve (solid blue line), after an initial mass loss, the curve remains constant without mass loss between 160 °C and 290 °C. For plasticized materials at different temperatures (TPS), the limits of the decomposition stages are found at higher temperatures than those of pure starch. The first stage, for instance, extends until temperatures of 290 °C. At this stage, the degradation occurs in two steps. Yunos and Rahman (2011) attribute this phenomenon to the effect of glycerol on starch-based polymers (Yunos & Rahman, 2011). For all processed TPS, the material loss due to evaporation of free water in the material occurs between 35 °C to 160 °C. In comparison, between 160 °C and 290 °C, it is considered that occurs the loss of the bound water of the material (Ismail et al., 2017; Paridah et al., 2016) together with the evaporation of the glycerol that starts at 200 °C and it ends around 300 ° C (Shi et al., 2007; Yunos & Rahman, 2011). In this way, in the first stage of thermal decomposition, the plasticizers (water and glycerol) are removed from the TPS structure during TGA heating.

In the second stage of thermal degradation, which takes place from 290 °C to 336 °C, the breakage of the starch chains and the glucose rings' oxidation occurs (Ismail et al., 2017). During the second stage, it is observed that TPS showed lower thermal stability than neat starch. This behavior has been ascribed to the ability of glycerol to reduce the inter-and intra-molecular bond interaction within the starchy polymeric matrix, which results in a decrease in the thermal stability of the material (Sessini et al., 2016). Finally, organic waste is degraded in the third thermal decomposition stage, and the residue is turned into ashes (Paridah et al., 2016).

The second and third stages of thermal decomposition are similar to all the studied TPS, with slight variations in the shape of the curve and the temperature ranges linked to the temperature profile at which they were processed. Finally, in Fig 6~~Fig 6~~-a, there is a very marked difference between the TPS studied and the pure starch due to the action of the plasticizer on the amylose and amylopectin chains, which gives it greater thermal resistance. In this way, from the shape of the TGA curve, it can be corroborated said that all the TPS formulations were plasticized to some degree despite the processing temperature. The formed materials can be classified into three groups if compared to starch: highly plasticized starch (T130 and T150), partially plasticized starch (T100 and T110), and incompletely plasticized (just a mixture of plasticizers and starch granules) (T70 and T90).

It is important to notice that in the case of T130 and T150, it can be observed that in the first stage, the loss of mass of these blends is less pronounced than in the other materials analyzed. To extend this observation, Table 4~~Table 4~~ reports the values for the onset decomposition temperature ($T_{5\%}$), the end decomposition temperature ($T_{90\%}$), and the temperature of the maximum decomposition rate (T_{max}).

Con formato: Fuente: Sin Negrita

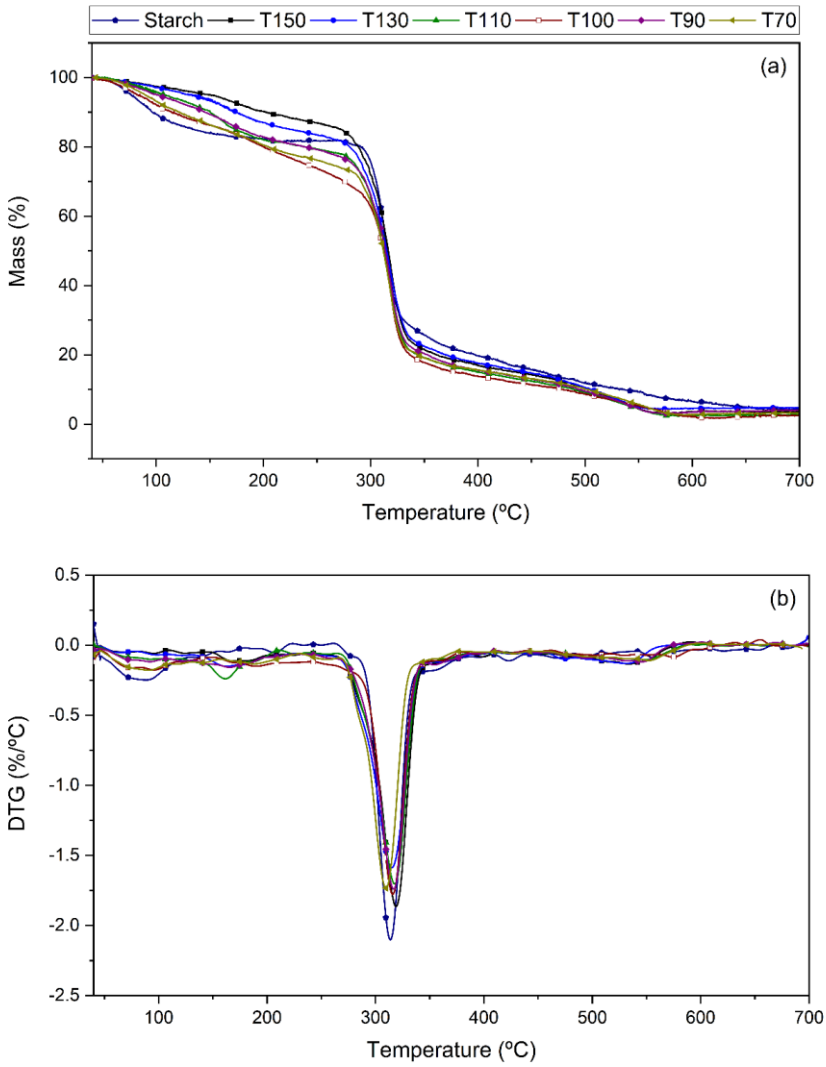

Fig 6 a) TGA and b) DTG curves of neat starch and obtained TPS at different extrusion temperature profiles

Table 4. Onset decomposition temperature ($T_{5\%}$), Temperature of maximum decomposition rate (T_{max}), and end decomposition temperature ($T_{90\%}$) for neat starch and the TPS obtained at different extrusion temperature profiles.

Sample label	$T_{5\%}$ (°C)	T_{max} (°C)	$T_{90\%}$ (°C)
Starch	76.6	314,5	532,7
T70	89.5	316.0	501.9
T90	100.7	317.1	494.6
T100	82.5	317.9	479.1
T110	107.7	319.6	489.6
T130	130.1	316.7	505.6
T150	150.5	317.6	504.2

In Table 4~~Table 4~~, based on the $T_{5\%}$ values, it is noted that the material's thermal stability increases with the increase in the extrusion temperature profile. An exception to this trend is the material processed at 100 °C (T100), in which the onset decomposition temperature is lower than the other studied formulations. This can be explained because of the water evaporation at the outlet of the extruder machine. The material becomes less thermally stable because the water reaches its boiling point and evaporates quickly from the polymeric matrix, thus generating a greater free volume and roughness within the material. In addition, there is less chance that water will completely gelatinize the starch matrix, making the material more susceptible to thermal degradation (Mitrus, 2009).

Con formato: Fuente: Sin Negrita

The increase in thermal stability confirms the TPS plasticization process. As discussed before, if the processing temperature profile increases, the granule breakage improves so that the number of starch granules that plasticize during the process increases. In this way, the starch chains tend to interact with each other, so high temperatures will be required to degrade the material structure, which results in a higher thermal resistance (Nafchi et al., 2013; Paridah et al., 2016). For T150, $T_{5\%}$ is around 15% and 60% higher than T130 and T70, respectively. This is ascribed to the recrystallized structures in the material, previously observed in SEM images (Fig 2~~Fig 2~~-g). These structures confer higher thermal stability since they require a higher temperature to degrade themselves, thus delaying the start of thermoplastic starch thermal decomposition. When the chain decomposition process begins in the second and third stages, no significant changes in T_{max} or $T_{90\%}$ for plasticized materials (TPS) were observed. This is because, after the plasticizers' evaporation (water and glycerol, from 290 °C), the composition of the materials is the same in all cases. However, for neat starch, the thermal stability is greater in these stages due to the granules not being subjected to disruption processes (extrusion and temperature), so it requires a higher temperature for its complete degradation, as shown in the $T_{90\%}$ value (Table 4~~Table 4~~.

Con formato: Fuente: Sin Negrita

Fig 7~~Fig 7~~ shows the differential scanning calorimetric curves obtained from the first and second DSC heating scan for the different TPS obtained at different processing temperatures. The glass transition temperature of TPS cannot be detected by this technique as no inflection point is observed in the obtained DSC curves. The TPS thermal transitions reported in the literature for starch-glycerol materials (Aldas, Pavon, et al., 2020a; Rodriguez-Gonzalez et al., 2004; Wattanakornsiri et al., 2012) are not easily observable by this technique. According to Averous and Boquillon (2004) and Averous et al. (2001), at the glass transition temperature, TPS presents a low drop in heat capacity, so it is sometimes challenging to detect the glass transition of this material using DSC analysis (Avérous et al., 2001; Averous & Boquillon, 2004). For the temperature range analyzed (-50 to 170 °C), the literature indicates that there is a thermal transition ascribed to the starch-rich phase (α relaxation), whose transition temperature (Tα) is between 34 and 70 °C and that it varies depending on the glycerol content and the moisture amount present in the material (Forssell et al., 2002; Wang & Huang, 2007b; Wattanakornsiri et al., 2012).

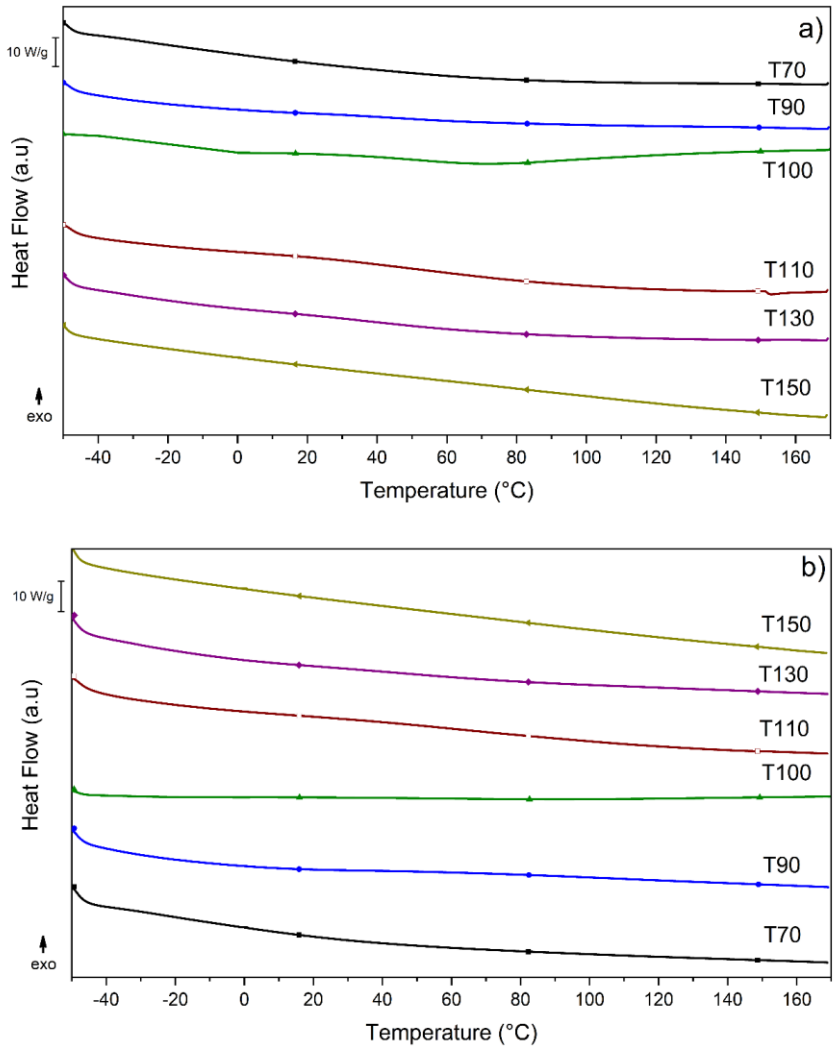

Fig 7 DSC a) first and b) second heating curves for TPS obtained at different extrusion temperature profiles

To verify the thermal transitions with a more accurate technique, the DTMA analysis was conducted (Averous & Boquillon, 2004). The variations of the loss factor (tan(δ)) and the storage modulus (G')

with temperature for all the studied materials are plotted in Fig 8~~Fig 8~~. The tan (δ) curves (Fig 8~~Fig 8~~-a) showed a heterogeneous system with two relaxations (peaks), between -60 °C and -40 °C and between 20 °C and 40 °C. The heterogeneity of the studied TPS is due to a phase separation with glycerol-rich domains (β relaxation) and starch-rich domains (α relaxation) (Enrione et al., 2010; Taguet et al., 2009). Therefore, each peak is so-called T_β and T_α, respectively, being T_β a secondary transition of TPS and T_α a primary transition of TPS (Taguet et al., 2009; Teixeira et al., 2012).

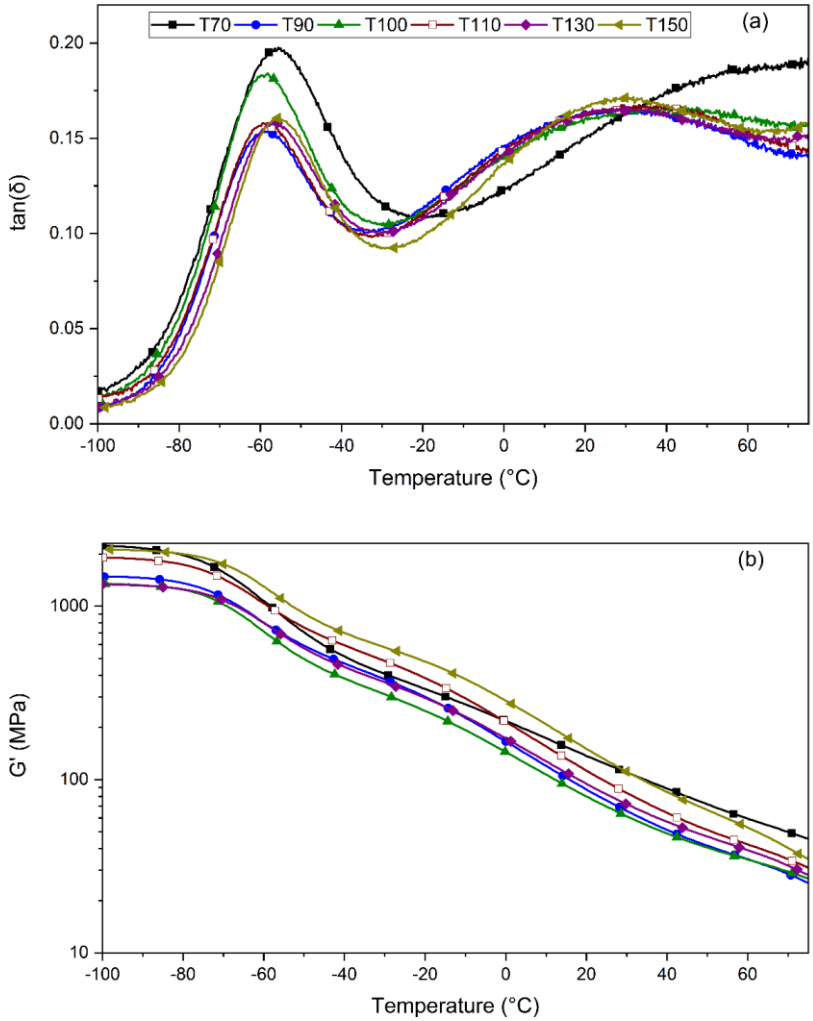

Fig 8 a) loss factor and b) storage modulus obtained from DMTA analysis for TPS containing 25 % glycerol and 10 % water processed at different temperature profiles

No differences were found in T_β (located at ~ -57 °C) and T_α (located at ~ 30 °C) of T90, T100, T110, T130, and T150. Notably, T70 shows a broader and poor unresolved T_α peak, and its T_β endset temperature is 10 °C higher than other TPS systems. This behavior confirms that starch was not completely plasticized at the temperature profile of 70 °C. Additionally, it can be concluded that at higher processing temperatures than 90 °C, the extrusion temperature profile has a negligible effect of on the TPS thermal transitions (T_α and T_β). The breadth of the T_α transition peak of Fig 8~~Fig 8~~-a of all the studied TPS is in good accordance with the literature (Averous & Boquillon, 2004; Wattanakornsiri et al., 2012). The broadness of the peaks points to a strong polydispersity in TPS due to different polymer chain lengths. Therefore, this explains the vague resolution of the thermal transitions in the DSC assessment and shows that this transition could only be observed with a DMTA analysis (Foreman, 2008).

Regarding the storage modulus (G') plotted in Fig 8~~Fig 8~~-b, the two identified relaxations, β and α relaxations, have two corresponding falls in the G' of the materials, at -63 °C and 25 °C, respectively. These falls show a reduction in TPS stiffness (Chartoff & Sircar, 2005). The G' curves show that from -100 °C to 25 °C, T150 has the highest storage modulus among the studied formulations. In temperatures above 30 °C, the G' of the T150 formulation constantly drops to similar values of the other formulations because the T_α was reached. Moreover, the storage modulus curve shows that T70 material does not lose G' as fast as the other formulations because the plasticization was not completely reached, and, consequently, the material does not have a thermoplastic behavior. The results confirm the good plasticization effect obtained for the extruded materials at temperatures above 100 °C, already discussed.

At 25 °C, T150 displays the highest storage modulus (117 MPa) followed by T110 (93 MPa) and T130 (80 MPa). However, the differences between the storage modulus of T110 and T130 is not too marked, as seen in the tensile test results T110 and T130 have statistically the same Young's modulus while T150 displays the higher value of them all and suggest a similar outcome in the storage modulus. T100 material presents a lower storage modulus (68MPa) than T110, T130, and T150 due to the limited resistance of its structure because of the formed holes. T70 and T90 are not completely plasticized materials and therefore their storage modulus cannot be compared with Young's modulus. These results agree with what the DRX patterns showed, an incomplete plasticization for T70 and T90, and a plasticized material for T100, T110, and T130. In this analysis is not possible to see the retrogradation of T150, however, it was vastly confirmed by previous analysis.

3.5. Water Uptake

Water absorption represents one of the most important characteristics of TPS-based products for many applications, i.e.: packaging, compostable agricultural films, and/or bags. The strong hydrogen bonds of starch hold the starchy polymeric chains together when submerged in water, making starch granules not soluble in cold water. Nevertheless, partial solubilization of starch is produced since the crystalline structure is disrupted in the TPS obtaining process, and water molecules are able to interact with the hydroxyl groups of amylose and amylopectin(Jiménez et al., 2012) and this is directly related to the water uptake of the TPS-based materials. Fig 9~~Fig 9~~ presents the different TPS water absorption curves. All the studied materials present a very fast initial water absorption within the first 15 minutes of the test. As Hoffman (2012) indicates, this behavior is explained by the hydrophilic nature of the materials used, starch and glycerol. In this way, the water that enters the material during the water uptake test interacts with the hydrophilic groups of thermoplastic starch, producing hydration of the system (Hoffman, 2012). After 15 minutes of testing, the behavior of the studied materials can be divided into three groups. First, the materials T90 and T70 presented a maximum water absorption of

37% at 15 and 30 minutes of testing, respectively. Both materials suffered ruptures of the test specimens due to swelling by water absorption. Then, T110 and T130 reached the water absorption equilibrium at 60% after 360 minutes (6 hours) of testing. These two formulations did not suffer breaks by swelling during the test. The third group is T100 and T150, which also failed (break by swelling) at 64 minutes with a water absorption percentage of 78% and 180 minutes with a water absorption percentage of 86%, respectively. The failures detected during the test in T70, T90, T100, and T150, occurred since after fast hydration of the TPS during the first 15 minutes, the water continues to enter the material and occupies the existing free volume between the chains. When the free volume is full, the chains reach a limit where they can no longer expand and, in turn, produce a general swelling of the material. But because of the osmotic force of the chains, the water continues to enter within the structure of the material, and it exceeds the existing free volume, which produces an over-swelling of the material structure and the consequent collapse of the system with a failure due to hydration (Hoffman, 2012; Neus Angles & Dufresne, 2000).

The diverse behavior of the materials detected for this test corroborates the influence of the extrusion temperature profile on the TPS plasticization process. On the one hand, the materials T70 and T90 had not achieved a complete plasticization of the starch, as previously discussed. For this reason, both formulations suffer failure of the material's structure prematurely during the water absorption. In the case of the T100 and T150 materials, whose structures were partially or fully plasticized as observed by SEM (Fig 2~~Fig 2~~-d and Fig 2~~Fig 2~~-g), the initial water absorption is higher than in the other TPS, reaching around 80%. This is explained since, in the T100 material, the structure presents porosities that facilitate water penetration and increase the free volume in the material, and it allows the fast entry of a greater quantity of water (Hoffman, 2012; Neus Angles & Dufresne, 2000). Nevertheless, these same holes decrease the swelling resistance so that the material structure collapses after 64 minutes of testing. In contrast, T150 absorbed water up to 86% of its weight since it presented a high elongation at break (as shown in the values in Table 4), which allowed a greater diffusion of water within its structure before breaking (Sen et al., 1998). The break by swelling of the material can be linked to the reduction in the mobility of the amylopectin chains in this TPS, which produce rigidity of the swollen material due to the formation of crystalline structures, previously discussed (see red arrows in Fig 2~~Fig 2~~-g) (Neus Angles & Dufresne, 2000). T110 and T130 have lower water absorption than T150 since they have a lower free volume. Still, at the same time, they are the only TPS formulations that reached the steady absorption state in which the material reaches the maximum water uptake (saturation level) without failure. This is because of the flexibility of the material's chains, which can recover their shape after maximum swelling (Chang et al., 2010). These results corroborate that T70 and T90 structures were incompletely plasticized, while T100, T110, T130, and T150 present plasticized structures, which agrees with the results of the other properties discussed previously.

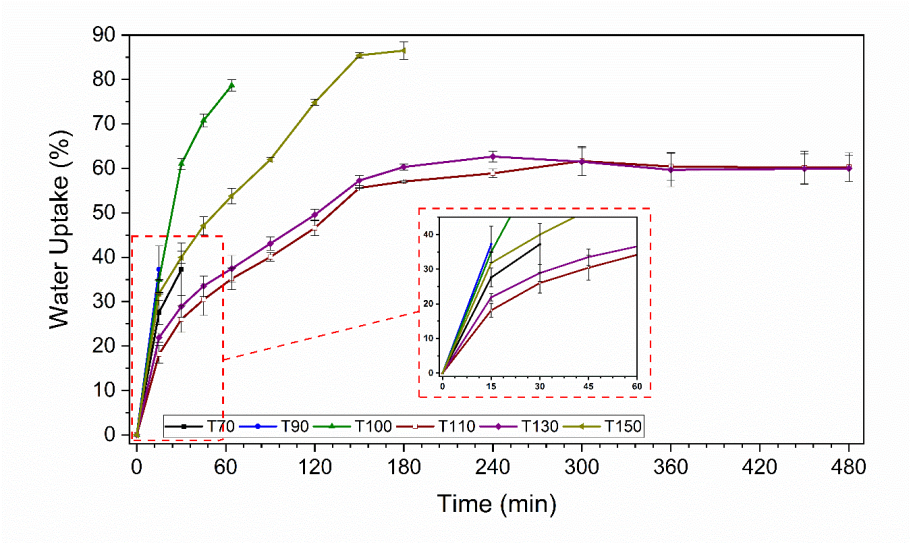

Fig 9 Water Uptake of TPS processed at different extrusion temperatures profiles

4. CONCLUSIONS

This work studied the effect of the extrusion temperature profile on the plasticization of native corn starch using water, and glycerol as plasticizers to obtain fully biobased and biodegradable thermoplastic starch by melt-extrusion simulating the industrial conditions for single-use plastic and packaging applications. With this purpose, this paper evaluated the thermal, mechanical, and microstructural characteristics of thermoplastic starch obtained at six different temperature profiles (T70, T90, T100, T110, T130 and T150) not only to find the best processing conditions for the obtention of food-grade TPS for scalable production at the industrial level, but also to understand the effect of the processing temperature on TPS-based materials final performance. SEM analysis showed that to produce a complete disruption of the starch granule, temperatures of 110 ºC or higher are needed. Materials obtained al 70 ºC and 90 ºC display poor mechanical behavior as they were not completely plasticized. Meanwhile, T100, T110, and T130 present plasticized structures. T100 presents porosity in its structure because water evaporation takes place at the extruder die, which affects its overall mechanical properties. T110 presents some residues of starch granules that point to a partial plasticization effect of the starchy structure. Moreover, even though T130 and T110 have statistically equal tensile moduli and tensile resistance, T130 presents a greater elongation at break than T110, which suggest that T130 has a higher degree of plasticization. T150 displays good mechanical properties but the material suffers thermal degradation as seen by its color change and the yellowish index. Moreover, T150 SEM images showed recrystallization and degradation due to the high-temperature processing conditions. Thermogravimetric analysis showed higher thermal stability in the TPS prepared at higher temperature profiles. DMTA test showed that at 25 °C the storage modulus of T150, T130, and T110 can correlate with Young's modulus. However, T100 presents a lower storage modulus because of the holes in its structure and, as T70 and T90 are not completely plasticized materials, these materials cannot be correlated with tensile modulus. Regarding water uptake, it was determined that water absorption is dependent on the plasticization of the structure, being T70 and T90 the materials with low water absorption and prone to premature rupture.

Meanwhile, T100, T110, T130, and T150 present high water absorption levels because the structure of the materials was partially or highly plasticized. The attained results allow concluding that there is a direct relationship between the TPS extrusion temperature profile used and the TPS overall performance. Glycerol and water can produce the starchy polymeric matrix transition from a glassy state to a thermoplastic state at temperatures between 110 and 130 ºC by using the melt-extrusion process, which is already established in the plastic processing industry, and allowing to obtain materials with good overall mechanical, thermal and able to withstand water absorption without the material breaking due to its swelling capacity. Finally, it can be concluded that the processing temperatures conditions of starchy-based materials clearly affect the final properties conferred by the plasticization of the thermoplastic starch structure and the study of different processing temperatures developed here opens the possibility of using these processing conditions at the industrial level.

Author contributions

Miguel Aldas: Methodology**,** Investigation, Writing - Review & Editing, Visualization; **Cristina Pavon:** Validation, Investigation, Formal analysis, Writing - Original Draft; **Harrison De La Rosa-Ramírez:** Methodology, Investigation; **Juan López-Martínez:** Funding acquisition, Resources, Supervision; **Marina P. Arrieta:** Conceptualization, Funding acquisition, Writing - Review & editing, Project administration

Funding

This research is a part of the grant PID2020-116496RB-C22 and PID2021-123753NA-C32 funded by MCIN/AEI/10.13039/501100011033 and by ERDF "A way of making Europe" by the "European Union" and by “Research Consolidation” Project (grant CNS2022-136064) funded by MCIN/AEI/10.13039/501100011033 and by the “European Union NextGenerationEU/PRTR”.

Acknowledgements

C.P. thanks Santiago Grisolía fellowship (GRISOLIAP/2019/113) from Generalitat Valenciana and Conselleria de Innovación, Universidades, Ciencia y Sociedad Digital (Regional Ministry of Innovation, Universities, Science and Digital Society) for the grant CIBEFP/2021/30. Microscopy Services at UPV are also acknowledged for their help in collecting and analyzing images.

STATEMENTS AND DECLARATIONS

Declaration of Competing Interest

The authors declare that they have no known competing financial interests or personal relationships that could have appeared to influence the work reported in this paper.

Data availability: The data presented in this study are available on request from the corresponding author

REFERENCES

Aldas, M., Ferri, J. M., Lopez-Martinez, J., Samper, M. D., & Arrieta, M. P. (2019). Effect of pine resin derivatives on the structural, thermal, and mechanical properties of Mater-Bi type bioplastic. *Journal of Applied Polymer Science*, *137*(4), 48236. https://doi.org/10.1002/app.48236

Aldas, M., Pavon, C., Ferri, J. M., Arrieta, M. P., & López-Martínez, J. (2021). Films Based on Mater-Bi® Compatibilized with Pine Resin Derivatives: Optical, Barrier, and Disintegration Properties. *Polymers*, *13*(9), 1506. https://doi.org/10.3390/polym13091506

Aldas, M., Pavon, C., López-Martínez, J., & Arrieta, M. P. (2020a). Pine resin derivatives as sustainable additives to improve the mechanical and thermal properties of injected moulded thermoplastic starch. *Applied Sciences (Switzerland)*, *10*(7). https://doi.org/10.3390/app10072561

Aldas, M., Pavon, C., López-Martínez, J., & Arrieta, M. P. P. (2020b). Pine resin derivatives as sustainable additives to improve the mechanical and thermal properties of injected moulded thermoplastic starch. *Applied Sciences*, *10*(7), 2561–2578. https://doi.org/10.3390/app10072561

Aldas, M., Rayón, E., López-Martínez, J., & Arrieta, M. P. (2020). A Deeper Microscopic Study of the Interaction between Gum Rosin Derivatives and a Mater-Bi Type Bioplastic. *Polymers*, *12*(1), 226–243. https://doi.org/10.3390/POLYM12010226

Angellier, H., Molina-Boisseau, S., Dole, P., & Dufresne, A. (2006). Thermoplastic Starch-Waxy Maize Starch Nanocrystals Nanocomposites. *Biomacromolecules*, *7*(2), 531–539. https://doi.org/10.1021/bm050797s

Apriyanto, A., Compart, J., & Fettke, J. (2022). A review of starch, a unique biopolymer – Structure, metabolism and in planta modifications. *Plant Science*, *318*, 111223. https://doi.org/10.1016/J.PLANTSCI.2022.111223

Arredondo Ochoa, T., García-Almendárez, B. E., Reyes, A. A., Pastrana, D. M. R., López, G. F. G., Belloso, O. M., & González, C. R. (2017). Design and Characterization of Corn Starch Edible Films Including Beeswax and Natural Antimicrobials. *Food and Bioprocess Technology*, *10*(1), 103–114. https://doi.org/10.1007/S11947-016-1800-4/FIGURES/7

Arrieta, M. P., Peltzer, M. A., Garrigós, M. D. C., & Jiménez, A. (2013). Structure and mechanical properties of sodium and calcium caseinate edible active films with carvacrol. *Journal of Food Engineering*, *114*(4), 486–494. https://doi.org/10.1016/J.JFOODENG.2012.09.002

Arrieta, M. P., Samper, M. D., Aldas, M., & López, J. (2017). On the Use of PLA-PHB Blends for Sustainable Food Packaging Applications. *Materials*, *10*(9). https://doi.org/10.3390/ma10091008

Artz, W. E., Warren, C., & Villota, R. (1990). Twin-Screw Extrusion Modification of a Corn Fiber and Corn Starch Extruded Blend. *Journal of Food Science*, *55*(3), 746–754. https://doi.org/10.1111/J.1365-2621.1990.TB05220.X

Averous, L., & Boquillon, N. (2004). Biocomposites based on plasticized starch: Thermal and mechanical behaviours. *Carbohydrate Polymers*, *56*(2), 111–122. https://doi.org/10.1016/j.carbpol.2003.11.015

Avérous, L., Fringant, C., & Moro, L. (2001). Plasticized starch-cellulose interactions in polysaccharide composites. *Polymer*, *42*(15), 6565–6572. https://doi.org/10.1016/S0032-3861(01)00125-2

Bastioli, C. (1998). Properties and applications of mater-Bi starch-based materials. *Polymer Degradation and Stability*, *59*(1–3), 263–272. https://doi.org/10.1016/S0141-3910(97)00156-0

Bertoft, E. (2017). Understanding starch structure: Recent progress. *Agronomy*, *7*(3). https://doi.org/10.3390/agronomy7030056

Campos, A., Teodoro, K. B. R., Teixeira, E. M., Corrêa, A. C., Marconcini, J. M., Wood, D. F., Williams, T. G., & Mattoso, L. H. C. (2013a). Properties of thermoplastic starch and TPS/polycaprolactone blend reinforced with sisal whiskers using extrusion processing. *Polymer Engineering and Science*, *53*(4), 800–808. https://doi.org/10.1002/pen.23324

Campos, A., Teodoro, K. B. R., Teixeira, E. M., Corrêa, A. C., Marconcini, J. M., Wood, D. F., Williams, T. G., & Mattoso, L. H. C. (2013b). Properties of thermoplastic starch and TPS/polycaprolactone blend reinforced with sisal whiskers using extrusion processing. *Polymer Engineering and Science*, *53*(4), 800–808. https://doi.org/10.1002/pen.23324

Castillo, L. A., López, O. V., García, M. A., Barbosa, S. E., & Villar, M. A. (2019). Crystalline morphology of thermoplastic starch/talc nanocomposites induced by thermal processing. *Heliyon*, *5*(6), e01877. https://doi.org/10.1016/J.HELIYON.2019.E01877

Chang, C., Duan, B., Cai, J., & Zhang, L. (2010). Superabsorbent hydrogels based on cellulose for smart swelling and controllable delivery. *European Polymer Journal*, *46*(1), 92–100. https://doi.org/10.1016/j.eurpolymj.2009.04.033

Chartoff, R., & Sircar, A. (2005). Thermal analysis of polymers. In *Encyclopedia of Polymer Science and Technology* (pp. 1–43).

Chen, J., Wang, X., Long, Z., Wang, S., Zhang, J., & Wang, L. (2020). Preparation and performance of thermoplastic starch and microcrystalline cellulose for packaging composites: Extrusion and hot pressing. *International Journal of Biological Macromolecules*, *165*, 2295–2302. https://doi.org/10.1016/j.ijbiomac.2020.10.117

Ciardelli, F., Bertoldo, M., Bronco, S., & Passaglia, E. (2019). The Obtainment of Bioplastics. In *Polymers from Fossil and Renewable Resources* (pp. 107–132). Springer International Publishing. https://doi.org/10.1007/978-3-319-94434-0_5

Costa, B. P., Carpiné, D., Ikeda, M., Alves, F. E. B. da S., de Melo, A. M., & Ribani, R. H. (2022). Developing a bioactive and biodegradable film from modified loquat (Eriobotrya japonica Lindl) seed starch. *Journal of Thermal Analysis and Calorimetry*, *147*(24), 14297–14313. https://doi.org/10.1007/S10973-022-11780-Z/TABLES/7

Dang, K. M., & Yoksan, R. (2015). Development of thermoplastic starch blown film by incorporating plasticized chitosan. *Carbohydrate Polymers*, *115*, 575–581. https://doi.org/10.1016/J.CARBPOL.2014.09.005

Enrione, J., Osorio, F., Pedreschi, F., & Hill, S. (2010). Prediction of the Glass Transition Temperature on Extruded Waxy Maize and Rice Starches in Presence of Glycerol. *Food and Bioprocess Technology*, *3*(6), 791–796. https://doi.org/10.1007/S11947-010-0345-1/TABLES/2

European Bioplastics. (2021). *Bioplastics market development*. http://www.european-bioplastics.org/news/publications/

European Commission. (2022). *European Commission. Commission Regulation (Eu) 2022/1616 of 15 September 2022 on Recycled Plastic Materials and Articles Intended to Come into Contact with Foods, and Repealing Regulation (Ec) No 282/2008 (Text with Eea Relevance)*.

European Commission. (2023). *Single-use plastics*. https://environment.ec.europa.eu/topics/plastics/single-use-plastics_en

Farokhi, M., Jonidi Shariatzadeh, F., Solouk, A., & Mirzadeh, H. (2019). Alginate Based Scaffolds for Cartilage Tissue Engineering: A Review. *Https://Doi.Org/10.1080/00914037.2018.1562924*, *69*(4), 230–247. https://doi.org/10.1080/00914037.2018.1562924

Ferri, J. M., Garcia-Garcia, D., Carbonell-Verdu, A., Fenollar, O., & Balart, R. (2018). Poly(lactic acid) formulations with improved toughness by physical blending with thermoplastic starch. *Journal of Applied Polymer Science*, *135*(4), 45751. https://doi.org/10.1002/app.45751

Foreman, J. (2008). Dynamic Mechanical Analysis of Polymers. In *Encyclopedia of Analytical Chemistry* (Issue January). https://doi.org/10.1002/9780470027318.a2007.pub2

Forssell, P. M., Mikkilä, J. M., Moates, G. K., & Parker, R. (2002). Phase and glass transition behaviour of concentrated barley starch-glycerol-water mixtures, a model for thermoplastic starch. *Carbohydrate Polymers*, *34*(4), 275–282. https://doi.org/10.1016/s0144-8617(97)00133-1

Gadhave, R. V, Das, A., Mahanwar, P. A., & Gadekar, P. T. (2018). Starch Based Bio-Plastics: The Future of Sustainable Packaging. *Open Journal of Polymer Chemistry*, *8*, 21–33. https://doi.org/10.4236/ojpchem.2018.82003

Ghanbari, A., Tabarsa, T., Ashori, A., Shakeri, A., & Mashkour, M. (2018). Preparation and characterization of thermoplastic starch and cellulose nanofibers as green nanocomposites: Extrusion processing. *International Journal of Biological Macromolecules*, *112*, 442–447. https://doi.org/10.1016/j.ijbiomac.2018.02.007

Gopi, S., Balakrishnan, P., Chandradhara, D., Poovathankandy, D., & Thomas, S. (2019). General scenarios of cellulose and its use in the biomedical field. *Materials Today Chemistry*, *13*, 59–78. https://doi.org/10.1016/J.MTCHEM.2019.04.012

Gopi, S., Pius, A., Kargl, R., Kleinschek, K. S., & Thomas, S. (2019). Fabrication of cellulose acetate/chitosan blend films as efficient adsorbent for anionic water pollutants. *Polymer Bulletin*, *76*(3), 1557–1571. https://doi.org/10.1007/S00289-018-2467-Y/TABLES/2

Hassan, M. M., Le Guen, M. J., Tucker, N., & Parker, K. (2019). Thermo-mechanical, morphological and water absorption properties of thermoplastic starch/cellulose composite foams reinforced with PLA. *Cellulose*, *26*(7), 4463–4478. https://doi.org/10.1007/s10570-019-02393-1

Hoffman, A. S. (2012). Hydrogels for biomedical applications. *Advanced Drug Delivery Reviews*, *64*, 18–23. https://doi.org/10.1016/j.addr.2012.09.010

Hoover, R. (2001). Composition, molecular structure, and physicochemical properties of tuber and root starches: a review. *Carbohydrate Polymers*, *45*(3), 253–267. https://doi.org/10.1016/S0144-8617(00)00260-5

Iaccheri, E., Siracusa, V., Ragni, L., De Aguiar Saldanha Pinheiro, A. C., Romani, S., Rocculi, P., Dalla Rosa, M., & Sobral, P. J. do A. (2023). Studying physical state of films based on casava starch and/or chitosan by dielectric and thermal properties and effects of pitanga leaf hydroethanolic extract. *Journal of Food Engineering*, *339*, 111280. https://doi.org/10.1016/J.JFOODENG.2022.111280

International Standards Organization. (2008). *ISO 62:2008 Plastics -- Determination of water absorption*.

Ismail, S., Mansor, N., & Man, Z. (2017). A Study on Thermal Behaviour of Thermoplastic Starch Plasticized by [Emim] Ac and by [Emim] Cl. *Procedia Engineering*, *184*, 567–572. https://doi.org/10.1016/j.proeng.2017.04.138

Jiménez, A., Fabra, M. J., Talens, P., & Chiralt, A. (2012). Edible and Biodegradable Starch Films: A Review. *Food and Bioprocess Technology 2012 5:6*, *5*(6), 2058–2076. https://doi.org/10.1007/S11947-012-0835-4

Jumaidin, R., Mohd Zainel, S. N., & Sapuan, S. M. (2020). Processing of Thermoplastic Starch. *Advanced Processing, Properties, and Applications of Starch and Other Bio-Based Polymers*, 11–19. https://doi.org/10.1016/B978-0-12-819661-8.00002-0

Jung, B. N., Kang, D. H., Shim, J. K., & Hwang, S. W. (2019). Physical and mechanical properties of plasticized butenediol vinyl alcohol copolymer/thermoplastic starch blend. *Journal of Vinyl and Additive Technology*, *25*(2), 109–116. https://doi.org/10.1002/vnl.21621

Kaseem, M., Hamad, K., & Deri, F. (2012). Thermoplastic starch blends: A review of recent works. *Polymer Science Series A*, *54*(2), 165–176. https://doi.org/10.1134/s0965545x1202006x

Lendvai, L., Sajó, I., & Karger-Kocsis, J. (2019). Effect of Storage Time on the Structure and Mechanical Properties of Starch/Bentonite Nanocomposites. *Starch - Stärke*, *71*(1–2), 1800123. https://doi.org/10.1002/STAR.201800123

Liu, W. C., Halley, P. J., & Gilbert, R. G. (2010). Mechanism of degradation of starch, a highly branched polymer, during extrusion. *Macromolecules*, *43*(6), 2855–2864. https://doi.org/10.1021/ma100067x

Ma, H., Qin, W., Guo, B., & Li, P. (2022). Effect of plant tannin and glycerol on thermoplastic starch: Mechanical, structural, antimicrobial and biodegradable properties. *Carbohydrate Polymers*, *295*, 119869. https://doi.org/10.1016/J.CARBPOL.2022.119869

Ma, X., & Yu, J. (2004). Formamide as the plasticizer for thermoplastic starch. *Journal of Applied Polymer Science*, *93*(4), 1769–1773. https://doi.org/10.1002/app.20628

Ma, X., Yu, J., He, K., & Wang, N. (2007). The Effects of Different Plasticizers on the Properties of Thermoplastic Starch as Solid Polymer Electrolytes. *Macromolecular Materials and Engineering*, *292*(4), 503–510. https://doi.org/10.1002/MAME.200600445

Marichelvam, Jawaid, & Asim. (2019). Corn and Rice Starch-Based Bio-Plastics as Alternative Packaging Materials. *Fibers*, *7*(4), 32. https://doi.org/10.3390/fib7040032

Mathew, A. P., & Dufresne, A. (2002). Plasticized waxy maize starch: Effect of polyols and relative humidity on material properties. *Biomacromolecules*, *3*(5), 1101–1108. https://doi.org/10.1021/bm020065p

Mendes, J. F., Paschoalin, R. T., Carmona, V. B., Sena Neto, A. R., Marques, A. C. P., Marconcini, J. M., Mattoso, L. H. C., Medeiros, E. S., & Oliveira, J. E. (2016). Biodegradable polymer blends based on corn starch and thermoplastic chitosan processed by extrusion. *Carbohydrate Polymers*, *137*, 452–458. https://doi.org/10.1016/j.carbpol.2015.10.093

Mitrus, M. (2005). Glass transition temperature of thermoplastic starches. *International Agrophysics*, *19*(3), 237–241. http://www.international-agrophysics.org/Glass-transition-temperature-of-thermoplastic-starches,106643,0,2.html

Mitrus, M. (2009). TPS and its nature. In L. P. B. M. Janssen & L. Moscicki (Eds.), *Thermoplastic Starch*. WILEY-VCH Verlag GmbH & Co. KGaA, Weinheim.

Mitrus, M., & Wojtowicz, Agnieszka Moscicki, L. (2009). Biodegradable Polymers and Their Practical Utility. In L. P. B. M. Janssen & L. Moscicki (Eds.), *Thermoplastic Starch*. WILEY-VCH Verlag GmbH & Co. KGaA, Weinheim.

Montilla-Buitrago, C. E., Gómez-López, R. A., Solanilla-Duque, J. F., Serna-Cock, L., & Villada-Castillo, H. S. (2021). Effect of Plasticizers on Properties, Retrogradation, and Processing of Extrusion-Obtained Thermoplastic Starch: A Review. *Starch - Stärke*, *73*(9–10), 2100060. https://doi.org/10.1002/STAR.202100060

Moro, T. M. A., Ascheri, J. L. R., Ortiz, J. A. R., Carvalho, C. W. P., & Meléndez-Arévalo, A. (2017). Bioplastics of Native Starches Reinforced with Passion Fruit Peel. *Food and Bioprocess Technology*, *10*(10), 1798–1808. https://doi.org/10.1007/S11947-017-1944-X/FIGURES/5

Nafchi, A. M., Moradpour, M., Saeidi, M., Alias, A. K., Mohammadi Nafchi, A., Moradpour, M., Saeidi, M., & Alias, A. K. (2013). Thermoplastic starches: Properties, challenges, and prospects. *Starch/Staerke*, *65*(1–2), 61–72. https://doi.org/10.1002/star.201200201

Neus Angles, M., & Dufresne, A. (2000). Plasticized starch/tuniein whiskers nanocomposites. 1. Structural analysis. *Macromolecules*, *33*(22), 8344–8353. https://doi.org/10.1021/ma0008701

Nevoralová, M., Koutný, M., Ujčić, A., Horák, P., Kredatusová, J., Šerá, J., Růžek, L., Růžková, M., Krejčíková, S., Šlouf, M., & Kruliš, Z. (2019). Controlled biodegradability of functionalized thermoplastic starch based materials. *Polymer Degradation and Stability*, *170*, 108995. https://doi.org/10.1016/J.POLYMDEGRADSTAB.2019.108995

Oniszczuk, T., & Janssen, L. P. B. M. (2009). Influence of Addition of Fiber on the Mechanical Properties of TPS Moldings. In *Thermoplastic Starch*. WILEY-VCH Verlag GmbH & Co. KGaA, Weinheim.

Ostafińska, A., Mikešová, J., Krejčíková, S., Nevoralová, M., Šturcová, A., Zhigunov, A., Michálková, D., & Šlouf, M. (2017). Thermoplastic starch composites with TiO2 particles: Preparation, morphology, rheology and mechanical properties. *International Journal of Biological Macromolecules*, *101*, 273–282. https://doi.org/10.1016/J.IJBIOMAC.2017.03.104

Paiva, D., Pereira, A. M., Pires, A. L., Martins, J., Carvalho, L. H., & Magalhães, F. D. (2018). Reinforcement of thermoplastic corn starch with crosslinked starch/chitosan microparticles. *Polymers*, *10*(9), 985. https://doi.org/10.3390/polym10090985

Paridah, M., Moradbak, A., Mohamed, A. Z., Owolabi, F. abdulwahab taiwo, Asniza, M., & Abdul Khalid, S. H. P. (2016). Thermoplastic Starch. In *Thermoplastic Elastomers*. https://doi.org/http://dx.doi.org/10.5772/57353

Pattanayaiying, R., Sane, A., Photjanataree, P., & Cutter, C. N. (2019). Thermoplastic starch/polybutylene adipate terephthalate film coated with gelatin containing nisin Z and lauric arginate for control of foodborne pathogens associated with chilled and frozen seafood. *International Journal of Food Microbiology*, *290*, 59–67. https://doi.org/10.1016/j.ijfoodmicro.2018.09.015

Pavon, C., Aldas, M., López-Martínez, J., Hernández-Fernández, J., & Patricia Arrieta, M. (2021). Films Based on Thermoplastic Starch Blended with Pine Resin Derivatives for Food Packaging. *Foods*, *10*(6), 1171. https://doi.org/10.3390/foods10061171

Pawlak, A., & Mucha, M. (2003). Thermogravimetric and FTIR studies of chitosan blends. *Thermochimica Acta*, *396*(1–2), 153–166. https://doi.org/10.1016/S0040-6031(02)00523-3

Pushpadass, H. A., Marx, D. B., & Hanna, M. A. (2008). Effects of extrusion temperature and plasticizers on the physical and functional properties of starch films. *Starch/Staerke*, *60*(10), 527–538. https://doi.org/10.1002/star.200800713

Rabe, S., Sanchez-Olivares, G., Pérez-Chávez, R., & Schartel, B. (2019). Natural keratin and coconut fibres from industrial wastes in flame retarded thermoplastic starch biocomposites. *Materials*, *12*(3), 344. https://doi.org/10.3390/ma12030344

Rayón, E., López-Martínez, J., & Arrieta, M. P. (2013). Mechanical characterization of microlaminar structures extracted from cellulosic materials using nanoindentation technique. *Cellulose Chemestry and Technology*, *47*, 345–351. https://www.researchgate.net/publication/258960193_Mechanical_characterization_of_microlaminar_structures_extracted_from_cellulosic_materials_using_nanoindentation_technique

Rodriguez-Gonzalez, F. J., Ramsay, B. A., & Favis, B. D. (2004). Rheological and thermal properties of thermoplastic starch with high glycerol content. *Carbohydrate Polymers*, *58*(2), 139–147. https://doi.org/10.1016/j.carbpol.2004.06.002

Romeira, K. M., Abdalla, G., Gonçalves, R. P., Pegorin, G. S., de Azeredo, H. M. C., Mussagy, C. U., & Herculano, R. D. (2021). Residual Starch Packaging Derived from Potato Washing Slurries to Preserve Fruits. *Food and Bioprocess Technology*, *14*(12), 2248–2259. https://doi.org/10.1007/S11947-021-02694-Z/FIGURES/7

Ruhul Amin, M., Anannya, F. R., Mahmud, M. A., & Raian, S. (2020). Esterification of starch in search of a biodegradable thermoplastic material. *Journal of Polymer Research*, *27*(1), 1–12. https://doi.org/10.1007/S10965-019-1983-2/TABLES/1

Scaffaro, R., Maio, A., & Lopresti, F. (2018). Physical properties of green composites based on poly-lactic acid or Mater-Bi® filled with Posidonia Oceanica leaves. *Composites Part A: Applied Science and Manufacturing*, *112*, 315–327. https://doi.org/10.1016/j.compositesa.2018.06.024

Schmitt, H., Guidez, A., Prashantha, K., Soulestin, J., Lacrampe, M. F., & Krawczak, P. (2015a). Studies on the effect of storage time and plasticizers on the structural variations in

thermoplastic starch. *Carbohydrate Polymers*, *115*, 364–372. https://doi.org/10.1016/j.carbpol.2014.09.004

Schmitt, H., Guidez, A., Prashantha, K., Soulestin, J., Lacrampe, M. F., & Krawczak, P. (2015b). Studies on the effect of storage time and plasticizers on the structural variations in thermoplastic starch. *Carbohydrate Polymers*, *115*, 364–372. https://doi.org/10.1016/J.CARBPOL.2014.09.004

Sen, M., Pekel, N., & Gu, O. (1998). Radiation synthesis and characterization of N-vinyl-2-pyrrolidone / N-allylthiourea hydrogels and their use in the adsorption of invertase. *Die Angewandte Makromolekulare Chemie*, *257*(4444), 1–6.

Sessini, V., Arrieta, M. P., Kenny, J. M., & Peponi, L. (2016). Processing of edible films based on nanoreinforced gelatinized starch. *Polymer Degradation and Stability*, *132*, 157–168. https://doi.org/10.1016/j.polymdegradstab.2016.02.026

Sessini, V., Arrieta, M. P., Raquez, J. M., Dubois, P., Kenny, J. M., & Peponi, L. (2019). Thermal and composting degradation of EVA/Thermoplastic starch blends and their nanocomposites. *Polymer Degradation and Stability*, *159*, 184–198. https://doi.org/10.1016/j.polymdegradstab.2018.11.025

Shi, R., Liu, Q., Ding, T., Han, Y., Zhang, L., Chen, D., & Tian, W. (2007). Ageing of Soft thermoplastic Starch with High Glycerol Content. *Journal of Applied Polymer Science*, *103*, 574–586. https://doi.org/10.1002/app

Souza, R. C. R., & Andrade, C. T. (2002a). Investigation of the gelatinization and extrusion processes of corn starch. *Advances in Polymer Technology*, *21*(1), 17–24. https://doi.org/10.1002/adv.10007

Souza, R. C. R., & Andrade, C. T. (2002b). Investigation of the gelatinization and extrusion processes of corn starch. *Advances in Polymer Technology*, *21*(1), 17–24. https://doi.org/10.1002/adv.10007

Stepto, R. F. T. (2006a). Understanding the Processing of Thermoplastic Starch. *Macromolecular Symposia*, *245–246*(1), 571–577. https://doi.org/10.1002/masy.200651382

Stepto, R. F. T. (2006b). Understanding the processing of thermoplastic starch. *Macromolecular Symposia*, *245–246*(1), 571–577. https://doi.org/10.1002/masy.200651382

Taguet, A., Huneault, M. A., & Favis, B. D. (2009). Interface/morphology relationships in polymer blends with thermoplastic starch. *Polymer*, *50*(24), 5733–5743. https://doi.org/10.1016/j.polymer.2009.09.055

Teixeira, E. de M., Curvelo, A. A. S., Corrêa, A. C., Marconcini, J. M., Glenn, G. M., & Mattoso, L. H. C. (2012). Properties of thermoplastic starch from cassava bagasse and cassava starch and their blends with poly (lactic acid). *Industrial Crops and Products*, *37*(1), 61–68. https://doi.org/10.1016/j.indcrop.2011.11.036

Thuwall, M., Boldizar, A., & Rigdahl, M. (2006). Extrusion processing of high amylose potato starch materials. *Carbohydrate Polymers*, *65*(4), 441–446.

Toro-Márquez, L. A., Merino, D., & Gutiérrez, T. J. (2018). Bionanocomposite Films Prepared from Corn Starch With and Without Nanopackaged Jamaica (Hibiscus sabdariffa) Flower

Comentado [MA3]: Esta dos veces esta referencia

Extract. *Food and Bioprocess Technology*, *11*(11), 1955–1973. https://doi.org/10.1007/S11947-018-2160-Z/FIGURES/7

Van Soest, J. J. G., De Wit, D., & Vliegenthart, J. F. G. (1996). Mechanical properties of thermoplastic waxy maize starch. *Journal of Applied Polymer Science*, *61*(11), 1927–1937. https://doi.org/10.1002/(sici)1097-4628(19960912)61:11<1927::aid-app7>3.0.co;2-l

Vinod, A., Sanjay, M. R., Suchart, S., & Jyotishkumar, P. (2020). Renewable and sustainable biobased materials: An assessment on biofibers, biofilms, biopolymers and biocomposites. *Journal of Cleaner Production*, *258*, 120978. https://doi.org/10.1016/J.JCLEPRO.2020.120978

Wang, H.-Y., & Huang, M. (2007a). Preparation, characterization and performances of biodegradable thermoplastic starch. *Polymers for Advanced Technologies*, *18*(April), 910–915. https://doi.org/10.1002/pat

Wang, H.-Y., & Huang, M. (2007b). Preparation, characterization and performances of biodegradable thermoplastic starch. *Polymers for Advanced Technologies*, *18*(April), 910–915. https://doi.org/10.1002/pat

Wattanakornsiri, A., Pachana, K., Kaewpirom, S., Traina, M., & Migliaresi, C. (2012). Preparation and Properties of Green Composites Based on Tapioca Starch and Differently Recycled Paper Cellulose Fibers. *Journal of Polymers and the Environment*, *20*(3), 801–809. https://doi.org/10.1007/s10924-012-0494-6

Wilpiszewska, K., & Spychaj, T. (2006). Heat plasticization of starch by extrusion in the presence of plasticizers. *Polimery*, *51*(05), 327–332. https://doi.org/10.14314/polimery.2006.327

Xie, F., Halley, P. J., & Avérous, L. (2012). Rheology to understand and optimize processibility, structures and properties of starch polymeric materials. *Progress in Polymer Science (Oxford)*, *37*(4), 595–623. https://doi.org/10.1016/j.progpolymsci.2011.07.002

Xie, F., Luckman, P., Milne, J., McDonald, L., Young, C., Tu, C. Y., Di Pasquale, T., Faveere, R., & Halley, P. J. (2014). Thermoplastic starch: Current development and future trends. *Journal of Renewable Materials*, *2*(2), 95–106. https://doi.org/10.7569/JRM.2014.634104

Yang, J. H., Yu, J. G., & Ma, X. F. (2006). A novel plasticizer for the preparation of thermoplastic starch. *Chinese Chemical Letters*, *17*(1), 133–136.

Ye, J., Hu, X., Luo, S., Liu, W., Chen, J., Zeng, Z., & Liu, C. (2018). Properties of Starch after Extrusion: A Review. *Starch - Stärke*, *70*(11–12), 1700110. https://doi.org/10.1002/STAR.201700110

Yunos, M. Z. B., & Rahman, W. A. W. A. (2011). Effect of Glycerol on Performance Rice Straw/Starch Based Polymer. *Journal of Applied Sciences*, *11*(13), 2456–2459.

Zhang, X., Ma, H., Qin, W., Guo, B., & Li, P. (2022). Antimicrobial and improved performance of biodegradable thermoplastic starch by using natural rosin to replace part of glycerol. *Industrial Crops and Products*, *178*, 114613. https://doi.org/10.1016/J.INDCROP.2022.114613

Zhang, Y., Rempel, C., & Liu, Q. (2014). Thermoplastic Starch Processing and Characteristics-A Review. *Critical Reviews in Food Science and Nutrition*, *54*(10), 1353–1370. https://doi.org/10.1080/10408398.2011.636156

Zhang, Y., Rempel, C., & McLaren, D. (2014). Thermoplastic Starch. In *Innovations in Food Packaging* (pp. 391–412). Academic Press. https://doi.org/10.1016/B978-0-12-394601-0.00016-3

Zullo, R., & Iannace, S. (2009). The effects of different starch sources and plasticizers on film blowing of thermoplastic starch: Correlation among process, elongational properties and macromolecular structure. *Carbohydrate Polymers*, *77*(2), 376–383. https://doi.org/10.1016/j.carbpol.2009.01.007